

Energetic Salts of the Binary 5-Cyanotetrazolate Anion ($[\text{C}_2\text{N}_5]^-$) with Nitrogen-Rich Cations

Margaret-Jane Crawford,^[a] Thomas M. Klapötke,^{*[a]} Franz A. Martin,^[a]
Carles Miró Sabaté,^{*[b]} and Magdalena Rusan^[a]

Abstract: The reaction of cyanogen (NC-CN) with MN_3 ($\text{M}=\text{Na}, \text{K}$) in liquid SO_2 leads to the formation of the 5-cyanotetrazolate anion as the monohemihydrate sodium ($1 \cdot 1.5\text{H}_2\text{O}$) and potassium (2) salts, respectively. Both $1 \cdot 1.5\text{H}_2\text{O}$ and 2 were used as starting materials for the synthesis of a new family of nitrogen-rich salts containing the 5-cyanotetrazolate anion and nitrogen-rich cations, namely ammonium (3), hydrazinium (4), semicarbazidium (5), guanidinium (6), aminoguanidinium (7), diaminoguanidinium (8), and triaminoguanidinium (9). Compounds $1-9$ were synthesised in good yields and characterised by using

analytical and spectroscopic methods. In addition, the crystal structures of $1 \cdot 1.5\text{H}_2\text{O}$, 2 , 3 , 5 , 6 , and $9 \cdot \text{H}_2\text{O}$ were determined by using low-temperature single-crystal X-ray diffraction. An insight into the hydrogen bonding in the solid state is described in terms of graph-set analysis. Differential scanning calorimetry and sensitivity tests were used to assess the thermal stability and sensitivity against impact and

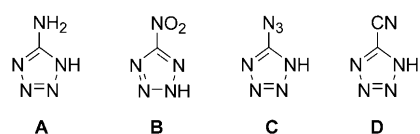
friction of the materials, respectively. For the assessment of the energetic character of the nitrogen-rich salts $3-9$, quantum chemical methods were used to determine the constant volume energies of combustion, and these values were used to calculate the detonation velocity and pressure of the salts using the EXPLO5 computer code. Additionally, the performances of formulations of the new compounds with ammonium nitrate and ammonium dinitramide were also predicted. Lastly, the ICT code was used to determine the gases and heats of explosion released upon decomposition of the 5-cyanotetrazolate salts.

Keywords: density functional calculations • energetic materials • nitrogen heterocycles • structure elucidation • X-ray diffraction

Introduction

Nitrogen-rich five-membered heterocycles are of considerable interest for the synthesis of energetic materials.^[1-3] This is due to a unique set of properties that such compounds possess. On the one hand, they are energetic due to the many C–N and N–N bonds they present,^[4] but on the other hand, they are thermally and chemically stable compounds with low sensitivities, due to the pseudoaromatic character of the heterocyclic ring.^[5]

In this context, Shreeve and co-workers recently published work on energetic nitrogen-rich salts and ionic liquids based on 5-amino-1*H*-tetrazole (**A**), which are promising for use as safe and “green” energetic materials for commercial applications.^[6] Although 5-nitro-2*H*-tetrazole (**B**) is extreme-



[a] Dr. M.-J. Crawford, Prof. Dr. T. M. Klapötke, F. A. Martin, M. Rusan
Department of Chemistry and Biochemistry
Energetic Materials Research
Ludwig-Maximilian University
Butenandstr. 5–13, 81377, Munich (Germany)
Fax: (+49) 89218077492
E-mail: tmk@cup.uni-muenchen.de

[b] Dr. C. Miró Sabaté
Laboratoire Hydrazines et Procédés
UMR 5179 CNRS-UCBL
Université Claude Bernard Lyon 1
Bat. Berthollet, 22 Av. Gaston Berger
69622 Villeurbanne (France)
Fax: (+33) 472431291
E-mail: carlos.miro-sabate@univ-lyon1.fr

Supporting information for this article is available on the WWW under <http://dx.doi.org/10.1002/chem.201002161>. This contains X-ray data tables, graph-set discussions, and tables of the explosive properties of mixtures of salts $3-9$ with ammonium nitrate and ammonium dinitramide.

ly sensitive towards impact and friction,^[7] nitrogen-rich salts based on the anion of **B** showed decreased sensitivities, and detonation parameters comparable to cyclotrimethylenetri-nitramine (RDX, Research Department Explosive).^[8] However, in comparison with **B** (anhydrous), alkali or transition-metal salts of **B** have sensitivities comparable to commonly used primary explosives, and might have potential as more environmentally friendly alternatives to lead(II) azide in initiating devices.^[9] In addition, a recent report from our group showed that both metal and nitrogen-rich salts of 5-azido-1*H*-tetrazole (**C**) are very powerful explosives. However, they are extremely sensitive compounds, which limits their field of application.^[10]

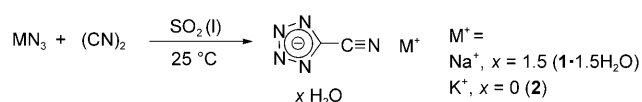
Within the field of energetic materials, nitrogen-rich compounds containing exclusively the elements C, H, and N might have potential for application as compounds with low flame temperatures, to increase the impulse in gun or rocket propellants, or as gas generators.^[11]

In this context, 5-cyanotetrazole (**D**) would be a good candidate for the synthesis of C-H-N-only compounds. The synthesis of **D** was first reported as early as 1912 by Passalacqua and Oliveri-Mandala,^[12] who treated hydrazoic acid (HN₃) with cyanogen (NC–CN). Several salts containing the 5-cyanotetrazolate anion and divalent transition metals (Mn²⁺, Fe²⁺, Ni²⁺, Co²⁺, and Cu²⁺) were reported by Franke and Groeneveld,^[13] and later on, Passmore and co-workers reported the synthesis and characterisation of the potassium and caesium salts of **D**, as well as the single-crystal structure of the caesium salt of **D**, namely Cs⁺[C₂N₅]⁻.^[14]

To our knowledge, the report on the caesium salt^[14] remains the only example of a 5-cyanotetrazolate salt that has been structurally characterised, and none of the compounds reported containing this anion have yet been considered as energetic materials. This prompted us to investigate the potential of salts of 5-cyanotetrazole with simple nitrogen-rich bases as energetic compounds. Consequently, we wish to present our work on the preparation, characterisation, and energetic testing of the sodium (**1**) and potassium (**2**) salts of 5-cyanotetrazole, as well as those of the nitrogen-rich ammonium (**3**), hydrazinium (**4**), semicarbazidium (**5**), guanidinium (**6**), aminoguanidinium (**7**), diaminoguanidinium (**8**), and triaminoguanidinium (**9**) derivatives.

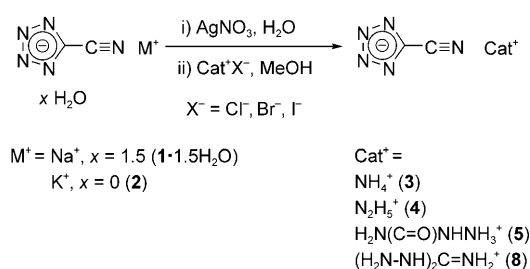
Results and Discussion

Synthesis and characterisation: The 5-cyanotetrazolate anion was synthesised by a [3+2] cycloaddition reaction of cyanogen (NC–CN) and one equivalent of a suitable metal azide (MN₃, M⁺=Na⁺, K⁺) in liquid sulfur dioxide to give the corresponding sodium and potassium salts, following the procedure of Passmore and co-workers.^[14] After washing the compounds out of the two-bulb flask used for their synthesis (see Supporting Information, Figure 1) with methanol/water and evaporating the solvent, the sodium salt was obtained as the monohemihydrate (**1**·1.5H₂O), and the potassium salt (**2**) was anhydrous (see Scheme 1).



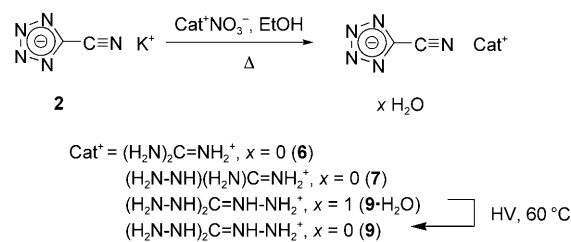
Scheme 1. Synthesis of sodium 5-cyanotetrazolate monohemihydrate (**1**·1.5H₂O) and potassium 5-cyanotetrazolate (**2**).

Both the sodium and the potassium salts (**1**·1.5H₂O or **2**) can be dissolved in distilled water and reacted with one equivalent of silver nitrate to precipitate silver 5-cyanotetrazolate. This latter compound was used in excess and reacted with a suitable halogenide salt in methanol to give the ammonium (**3**), hydrazinium (**4**), semicarbazidium (**5**), and diaminoguanidinium (**8**) salts of 5-cyanotetrazole, as presented in Scheme 2.



Scheme 2. Synthesis of ammonium (**3**), hydrazinium (**4**), semicarbazidium (**5**), and diaminoguanidinium (**8**) 5-cyanotetrazolate.

For **6**, **7**, and **9** the potassium salt (**2**) was heated at reflux in ethanol with an equivalent amount of the corresponding nitrate salt. After work-up, the guanidinium (**6**) and aminoguanidinium (**7**) salts were obtained as anhydrous materials, whereas the triaminoguanidinium compound was obtained as a monohydrate (**9**·H₂O, see Scheme 3). The water of crys-



Scheme 3. Synthesis of guanidinium (**6**), aminoguanidinium (**7**), and triaminoguanidinium (**9**·H₂O and **9**) 5-cyanotetrazolate salts. HV = high vacuum.

tallisation in triaminoguanidinium 5-cyanotetrazolate monohydrate (**9**·H₂O) can be conveniently removed by heating the compound under high vacuum to yield the anhydrous species (**9**) in quantitative yield.

Compounds **1–9** were characterised by analytical (elemental analysis and mass spectrometry) and spectroscopic (IR, Raman, and NMR) methods. In addition, the crystal struc-

tures of salts **1**·1.5H₂O, **2**, **3**, **5**, **6**, and **9**·H₂O were determined by low-temperature X-ray diffraction techniques.

NMR spectroscopy: The $^{13}C\{^1H\}$ NMR spectra of all compounds were measured in $[D_6]DMSO$, and show two resonances at $\delta = 137.8$ and 115.1 ppm, which can be attributed to the signals of the carbon atom of the tetrazolate ring and CN group, respectively. In the ^{14}N NMR spectra, two broad resonances ($\nu_{1/2} \approx 400$ Hz) at $\delta \approx +20$ and ≈ -50 ppm were observed, corresponding to the nitrogen atoms labelled as N3/4 and N2/5 (X-ray labels) in the tetrazolate ring. In the ^{14}N NMR spectra of the 5-cyanotetrazolate salts, the resonance due to the nitrogen atom in the CN group is observed in all compounds at $\delta \approx -120$ ppm ($\nu_{1/2} \approx 600$ Hz). In addition to the resonances corresponding to the anion, compounds **5–9** exhibit resonances at $\delta \approx 159.0$ ppm in the $^{13}C\{^1H\}$ NMR spectra which are absent in the $^{13}C\{^1H\}$ NMR spectra of **1** and **2**, indicating that these can be attributed to the central carbon atom of the cations. The ^{14}N NMR spectrum of the guanidinium salt **6** shows an additional resonance at $\delta = -311$ ppm, corresponding to the nitrogen atoms of the three NH₂ groups. In the amino-, diamino-, and triaminoguanidinium salts (**7–9**, respectively) the resonance of the NH/NH₂ groups shifts to higher field with an increasing number of NH₂ groups in the molecule; thus, compound **7** shows a signal at $\delta = -319$ ppm, which is shifted to $\delta = -375$ ppm in **8**, and to $\delta = -397$ ppm in **9**.

Furthermore, on exchanging the metal cations in **1** and **2** for nitrogen-rich cations, no significant changes in the $^{13}C\{^1H\}$ or ^{14}N NMR chemical shifts corresponding to the 5-cyanotetrazolate anion are observed.

Vibrational spectroscopy: Salts **1–9** were identified by infrared (IR) and Raman (Ra) spectroscopy. The vibrations corresponding to the ammonium, hydrazinium, semicarbazidium, guanidinium, aminoguanidinium, and triaminoguanidinium cations in compounds **3–9** have been described previously, and therefore a detailed discussion is omitted from this work.^[8,15] To establish a characteristic set of vibrations for the 5-cyanotetrazolate anion, its vibrational frequencies were calculated by quantum chemical methods (see Experimental Section for details of the method used). The quantum chemical calculations facilitated the assignment of the anion bands observed in the vibrational spectra of **1–9**, and provided structural information about the 5-cyanotetrazolate anion in the gaseous state. The scaled (calculated) IR and

Raman frequencies, and the calculated IR intensities and Raman activities, are summarised in Table 1, along with the averaged measured frequencies, qualitative IR intensities, and averaged Raman activities (quantitative) observed experimentally in the vibrational spectra of compounds **1–9**. The experimentally observed vibrations can thus be assigned by comparison with the computed values. All 15 frequencies obtained from the computational results match the experimentally observed values fairly well for salts **1–9**. The rather similar vibration frequencies observed for the anions of compounds **1–9** suggest strong similarities in their solid state geometries, as confirmed by X-ray studies (see discussion below and Supporting Information, Table 1).

The most intense band in the Raman/IR spectra of all salts is found fairly consistently at $\approx 2265/2260$ cm⁻¹, corresponding to the N1–C1 (see X-ray labels) stretching vibration of the CN group in the anion. The strong bands occurring at ≈ 1410 (Raman)/1415 cm⁻¹ (IR) can be attributed to the C2–(N2/N5) asymmetric stretching vibration of the 5-cyanotetrazolate anion. The stretching vibration of the N3–N4 bond in the anion is observed as an absorption band at ≈ 1205 cm⁻¹ (both Raman and IR). Whereas the symmetric stretching vibration of the N2–N3 and N4–N5 bonds in the anion are apparent from a band of medium intensity at 1065 cm⁻¹ (both Raman and IR), the asymmetric stretching vibration is shifted to ≈ 1190 cm⁻¹ (Raman) and ≈ 1185 cm⁻¹ (IR). In addition to the bands of lower intensity corresponding to vibrational modes in the anion, compounds **3–9** show bands in the range 3400 – 3330 and 1295 – 1145 cm⁻¹, which are due to the asymmetric stretching of the NH₂ groups and the rocking/twisting vibrational modes of the NH₂ groups, respectively.^[6d,16]

Crystal structures: Single crystals of compounds **1**·1.5H₂O, **2**, **3**, **5**, **6**, and **9**·H₂O were grown as described in the Experi-

Table 1. Calculated, scaled, and measured IR and Raman frequencies with intensity (IR) and activity (Raman) values for the 5-cyanotetrazolate anion.

| | ν_{scal} [cm ⁻¹] ^[a] | I_{calcd} IR/Raman ^[b] | ν_{meas} (IR) [cm ⁻¹] ^[c] | ν_{meas} (Raman) [cm ⁻¹] ^[d] | Mode assignment ^[e] |
|----|---|---|--|---|---|
| 1 | 179 | 9/0.19 | | n.o. | ω (ring) |
| 2 | 187 | 6/2 | | 210 | τ (C1–N1) |
| 3 | 508 | 5/2 | 495 | 495 | γ (N1–C1–C2) |
| 4 | 543 | 3/0.02 | 545 | 540 | δ (N1–C1–C2) |
| 5 | 576 | 4/8 | 600 | n.o. | ν (C1–C2) & ω (ring) |
| 6 | 713 | 0/0.004 | n.o. | 715 | γ (N–N–N) _{ring} “out-of-phase” |
| 7 | 718 | 2/0.5 | 735 | 735 | γ (N2–C2–N5) “out-of-phase” |
| 8 | 1005 | 2/38 | 1020 | n.o. | ν_s (N–N) _{ring} |
| 9 | 1009 | 2/0.05 | 1050 | 1010 | δ (N2–N3–N4) |
| 10 | 1029 | 5/11 | 1080 | n.o. | δ (N2–C2–N5) |
| 11 | 1131 | 8/3 | 1150 | n.o. | ν_{as} (N–N) _{ring} & ν_{as} (C–N) _{ring} |
| 12 | 1158 | 13/6 | 1185 | 1155 | ν_s (N–N) _{ring} & ν_s (C–N) _{ring} |
| 13 | 1319 | 33/0.006 | 1365 | n.o. | ν_s (N2–C2–N5) “in-phase” |
| 14 | 1363 | 1/69 | 1385 | 1370 | ν (C1–C2) |
| 15 | 2215 | 165/408 | 2260 | 2260 | ν (C1–N1) |

[a] Calculated frequencies (B3-LYP/6-31G(d))^[17] scaled by 0.9613.^[18] [b] Calculated IR intensities and Raman activities. [c] Experimental IR frequencies and intensities. [d] Experimental Raman frequencies and activities in parentheses. [e] Approximate description of vibrational modes: ν = stretching, δ = in-plane bending, γ = out-of-plane bending, ω = in-plane rocking, τ = torsion; as = asymmetric; and s = symmetric.

mental Section. The X-ray crystallographic data for salts **1**·1.5H₂O, **2**, **3**, **5**, **6**, and **9**·H₂O were collected on an Oxford Diffraction Xcalibur 3 diffractometer equipped with a CCD detector using graphite-monochromated MoK α radiation ($\lambda = 0.71073 \text{ \AA}$). The structures were solved with SHELXS-97, and were refined by means of full-matrix least-squares procedures using SHELXL-97,^[19,20] implemented in the package WinGX,^[21] and finally checked using Platon.^[22] For all the structures all hydrogen atoms were refined isotropically. The crystallographic data are summarised in Table 2. Selected bond lengths and angles are reported in Table 1 of the Supporting Information. In addition, the coordination around the metal cations in salts **1**·1.5H₂O and **2**, the hydrogen-bonding geometries, and the results of the graph-set analysis are available in the Supporting Information (Tables 2–9). CCDC-784022 (**1**·1.5H₂O), 784020 (**2**), 784021 (**3**), 784023 (**5**), 784019 (**6**), and 784024 (**9**·H₂O) contain the supplementary crystallographic data for this paper. These data can be obtained free of charge from The Cambridge Crystallographic Data Centre via www.ccdc.cam.ac.uk/data_request/cif.

The two hydrated compounds in this work (i.e., **1**·1.5H₂O and **9**·H₂O) both crystallise in triclinic systems in the space group $P\bar{1}$, whereas **2**, **3**, **5**, and **6** all have monoclinic cells. The cells of salts **2** and **5** belong to the space group $C2/c$, whereas those of compounds **3** and **6** are of type $P2_1/c$.

The sodium salt crystallises incorporating 1.5 molecules of crystal water per formula unit (**1**·1.5H₂O) with $Z = 2$ and $V = 599.1(1) \text{ \AA}^3$. Figure 1 shows the coordination environment of the two crystallographically inequivalent Na⁺ ions (Na1 and Na2) and the corresponding labelling scheme. The distance between Na1 and Na2 is 3.523(1) Å, and the Na⁺

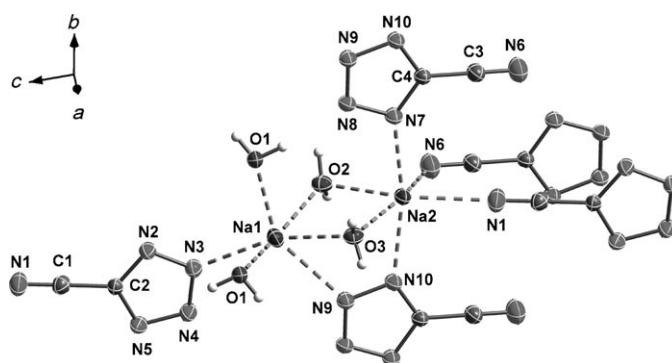


Figure 1. Coordination environment of the two Na⁺ ions in **1**·1.5H₂O, and labelling scheme (diamond plot with thermal ellipsoids at 50% probability).

ions are linked to each other by coordination to water molecules with $d_{\text{Na-O2}}$ and $d_{\text{Na-O3}} \approx 2.4 \text{ \AA}$, and through N9 and N10 of one tetrazolate ring with $d_{\text{Na1-N9}} = 2.738(1)$ and $d_{\text{Na2-N10}} = 2.433(1) \text{ \AA}$. Table 2 of the Supporting Information summarises the parameters corresponding to the coordination around the two metal centres. Both Na⁺ ions have a coordination number of six, which is completed either by interactions with four water molecules and two anions (Na1), or with four anions and two water molecules (Na2), forming a distorted octahedron in both cases. All contact distances are in the range $\approx 2.4\text{--}2.7 \text{ \AA}$, which are comparable with other salts in which a sodium cation is coordinated to oxygen or nitrogen atoms.^[9a,23,24]

The presence of water in the solid-state structure of **1**·1.5H₂O does not allow the compound to form planar

Table 2. Crystal structure solution and refinement for 5-cyanotetrazolate salts **1**·1.5H₂O, **2**, **3**, **5**, **6**, and **9**·H₂O.

| Parameter | 1 ·1.5H ₂ O | 2 | 3 | 5 | 6 | 9 ·H ₂ O |
|--|--|---------------------------------|--|--|--|--|
| formula | C ₂ H ₃ N ₅ O _{1.5} Na | C ₂ N ₄ K | C ₂ H ₄ N ₆ | C ₃ H ₆ N ₈ O | C ₃ H ₆ N ₈ | C ₃ H ₁₁ N ₁₁ O |
| M_r | 144.08 | 133.17 | 112.11 | 170.16 | 154.16 | 217.23 |
| crystal system | triclinic | monoclinic | monoclinic | monoclinic | monoclinic | triclinic |
| space group | $P\bar{1}$ | $C2/c$ | $P2_1/c$ | $C2/c$ | $P2_1/c$ | $P\bar{1}$ |
| a [Å] | 6.780(1) | 7.775(5) | 3.7801(1) | 11.1655(7) | 3.6733(1) | 6.6838(5) |
| b [Å] | 7.064(1) | 10.276(5) | 14.0833(4) | 10.0335(4) | 11.5516(3) | 7.9159(5) |
| c [Å] | 12.783(1) | 6.769(5) | 9.4141(3) | 14.1418(8) | 16.6453(5) | 10.2312(7) |
| α [°] | 101.01(1) | 90 | 90 | 90 | 90 | 73.09(1) |
| β [°] | 94.21(1) | 121.7(1) | 97.507(3) | 110.230(6) | 92.778(3) | 88.94(1) |
| γ [°] | 90.71(1) | 90 | 90 | 90 | 90 | 68.96(1) |
| V [Å ³] | 599.1(1) | 460.0(2) | 496.88(2) | 1486.6(1) | 705.47(3) | 481.1(2) |
| Z | 2 | 4 | 4 | 8 | 4 | 2 |
| ρ_{calcd} [g cm ⁻³] | 1.597 | 1.923 | 1.499 | 1.521 | 1.451 | 1.499 |
| μ (MoK α) [cm ⁻¹] | 0.192 | 1.018 | 0.115 | 0.122 | 0.111 | 0.120 |
| $F(000)$ [e] | 292 | 264 | 232 | 704 | 320 | 228 |
| hkl range | $\pm 9, \pm 9, \pm 18$ | $\pm 9, \pm 12, \pm 8$ | $\pm 4, \pm 17, \pm 11$ | $\pm 13, \pm 12, \pm 17$ | $\pm 4, \pm 14, \pm 20$ | $\pm 8, \pm 9, \pm 12$ |
| $((\sin\theta)/\lambda)_{\text{max}}$ [Å ⁻¹] | 30.1 | 26.0 | 27.0 | 26.0 | 26.0 | 26.0 |
| measured reflns | 8176 | 2234 | 5186 | 7076 | 7001 | 4912 |
| unique reflns | 3486 | 454 | 1077 | 1460 | 1385 | 1883 |
| R_{int} | 0.0365 | 0.0578 | 0.0298 | 0.0597 | 0.0263 | 0.0181 |
| parameters | 196 | 39 | 89 | 133 | 124 | 180 |
| $R(F)/wR(F^2)$ [all reflns] | 0.0604/0.0948 | 0.0335/0.0699 | 0.0422/0.0792 | 0.0701/0.0875 | 0.0374/0.0796 | 0.0411/0.0889 |
| GOF (F^2) ^[a] | 1.001 | 1.212 | 1.080 | 0.939 | 1.086 | 1.060 |
| $\Delta\rho_{\text{min}}$ (max/min) [e Å ⁻³] | -0.23/0.22 | -0.36/0.28 | -0.19/0.17 | -0.19/0.19 | -0.18/0.12 | -0.18/0.20 |

[a] $R_1 = \sum ||F_o| - |F_c|| / \sum |F_o|$; $R_w = [\sum (F_o^2 - F_c^2)^2 / \sum w(F_o^2)]^{1/2}$; $w = [\sigma_c^2(F_o^2) + (xP)^2 + yP]^{-1}$, $P = (F_o^2 - 2F_c^2)/3$.

layers when packing, and waves are formed instead. There are no significant interactions between the waves, and the shortest distance between two waves is 3.384(2) Å. Figure 2

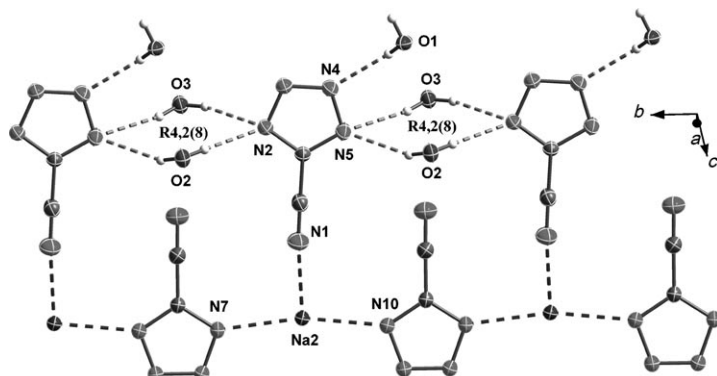


Figure 2. Infinite chains in the crystal structure of $1 \cdot 1.5H_2O$ connected by hydrogen bonds and coordination to the Na^+ ions.

shows a view of one of the wave layers observed in the crystal structure of $1 \cdot 1.5H_2O$. The CN groups in the anions point in opposite directions, approximately parallel to the c axis. The anions that are oriented towards negative values of the axis ($-c$) are linked by Na^+ ions with $d_{Na-N} \approx 2.4$ Å, and form infinite chains along the b axis. The anions with the CN groups pointing in the $+c$ direction are linked together by hydrogen bonds with O2 and O3 of the two water molecules, with distances between donor and acceptor $d_{O-N} \approx 2.9$ – 3.1 Å (see Supporting Information, Table 4). N4 is involved in the formation of a third hydrogen bond to O1 with $d_{O1-N4(iii)} = 2.894(2)$ Å (symmetry code: iii: $x, 1+y, z$), whereas N1 and N3 interact with Na2 and Na1, respectively.

Compound **2** crystallises with a density of 1.923 g cm^{-3} in a structure which forms planar layers. The atoms on the 5-cyanotetrazolate anion lie on a two-fold axis parallel to the axis that bisects the anions along the linear $C-C\equiv N$ bonds, making the two halves of the anion identical. The structure is very similar to that of the previously reported caesium salt.^[14] The cell parameters a and b are, as expected, slightly shorter than for the caesium salt (≈ 0.5 and ≈ 0.7 Å shorter, respectively), due to the smaller size of K^+ in comparison to Cs^+ . However, the c dimension ($6.769(5)$ Å) changes very little with respect to the caesium compound ($6.983(2)$ Å), because the layers are formed on the ab plane, and there is more space between the layers to accommodate a larger cation. The separation between layers in the potassium salt is exactly $c/2$ (i.e., 3.39 Å).

Each K^+ ion has contacts with nine nitrogen atoms from six different anions (see Figure 3), a common coordination number for potassium salts.^[9a,25] The Coulombic interactions between the potassium cations and the nitrogen atoms (see Supporting Information, Table 3), in the range between $2.871(3)$ and $3.098(2)$ Å, are shorter than, or very similar to, the sum of the ionic radii of K^+ (1.33 Å) and nitrogen (1.71 Å).^[26]

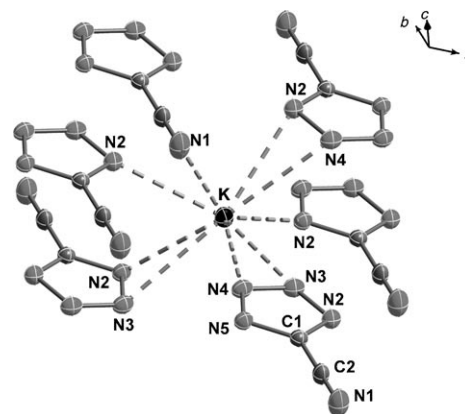


Figure 3. Coordination environment of the K^+ ion in **2** and labelling scheme (diamond plot with thermal ellipsoids at 50% probability).

The absence of crystal water in the compound results in marked differences in the packing of **2** in comparison with the sodium salt ($1 \cdot 1.5H_2O$). Five of the nine cation–anion contacts link the cations and anions into sheets parallel to the ab -plane (see Figure 4), with the C_2 fold axis oriented

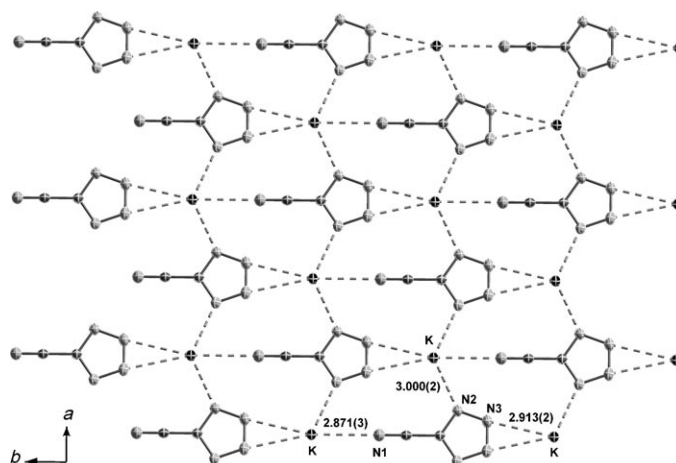


Figure 4. Interactions between the K^+ ions and the anions in **2** within sheets parallel to the ab plane.

parallel to the b axis. The remaining three interactions between K^+ and the anions link adjacent sheets, so that the anions form stacks and the K^+ ions form channels; these are parallel to the c axis, with the CN groups on the anions in adjacent sheets pointing in opposite directions parallel to the b axis. The unit cell contains four halves of K^+ ions, two whole K^+ ions, and 5-cyanotetrazolate anions, so that $Z=4$. Figure 5 is a schematic view of the three-dimensional array formed by the K^+ ions. The hexagonal channels are occupied by K^+ ions and contain the anion stacks described above. The metal centres are tetrahedrally coordinated, with two shorter (3.986 Å) and two longer (4.681 Å) interactions forming a lattice identical to that of diamond. Note

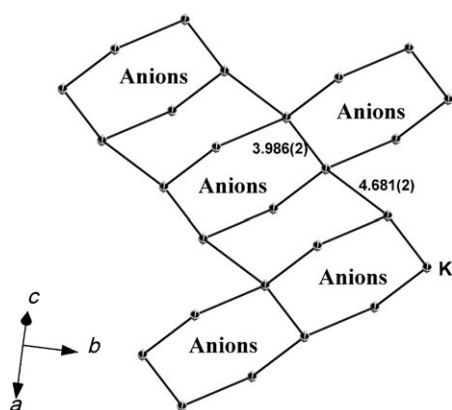


Figure 5. Tetrahedral (diamond-like) lattice formed by the K^+ ions in **2**. The cations form hexagonal channels, which are occupied by the anions (the lattice formed by the anions is identical, with K^+ ions occupying the hexagonal channels).

that the same type of hexagonal channel is formed by the anions, with the metal occupying the voids.

Figure 6 shows a view of the unit cell of compound **3** with extensive hydrogen bonding. Apart from the nitrogen atom labelled as N3, all nitrogen and hydrogen atoms in the mole-

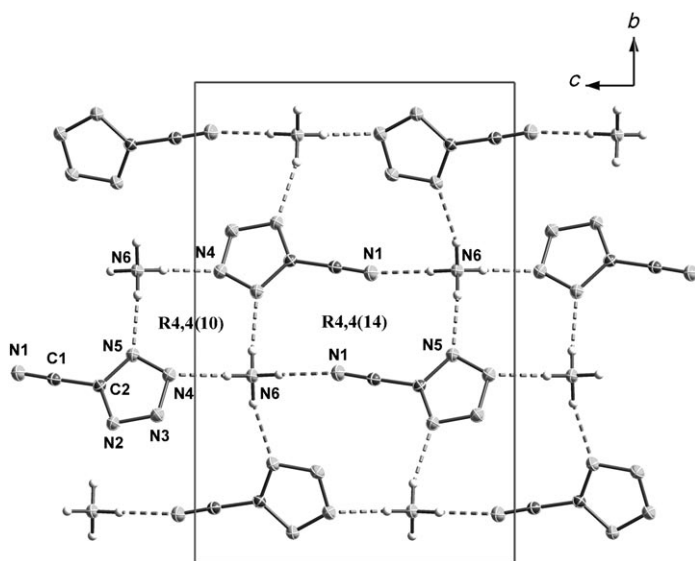


Figure 6. Hydrogen bonding in the unit cell of **3** and labelling scheme (diamond plot with thermal ellipsoids at 50% probability).

cule participate in the formation of medium-to-strong hydrogen bonds (Supporting Information, Table 4), with distances between donor and acceptor atoms < 3 Å. The primary hydrogen-bonding graph-set (Supporting Information, Table 6) is described by four dimeric interactions with N6 of the ammonium cation as the donor atom ($N_1 = 4\text{-D1,1(2)}$), which combine at the secondary level to form chain motifs of different sizes (two $C2,2(6)$, one $C2,2(7)$, and one $C2,2(8)$). In addition, two ring patterns are formed: an

$R4,4(10)$ graph-set starting at N6 and finishing at $N3^{iii}$ (symmetry code: iii: $-x, 1-y, 1-z$) and an $R4,4(14)$ network going from N6 to $N4^{iv}$ (symmetry code: (iv) $1+x, 1+y, z$). Both patterns are represented in Figure 6.

Compound **5** has a relatively high density ($D_{\text{calcd}} = 1.521 \text{ g cm}^{-3}$) in comparison to the other 5-cyanotetrazolate salts in this study. The positive charge is located mainly on the nitrogen atom labelled crystallographically as N8, and there is a planar arrangement of the non-hydrogen atoms in the cation. There is extensive hydrogen bonding in the crystal structure, as shown by a view of the unit cell along the b axis (Figure 7). The semicarbazidium cations form planar layers along a direction which cuts the a - and c -axes at an angle of $\approx 45^\circ$, whereas the 5-cyanotetrazolate anions form non-planar layers along the c axis.

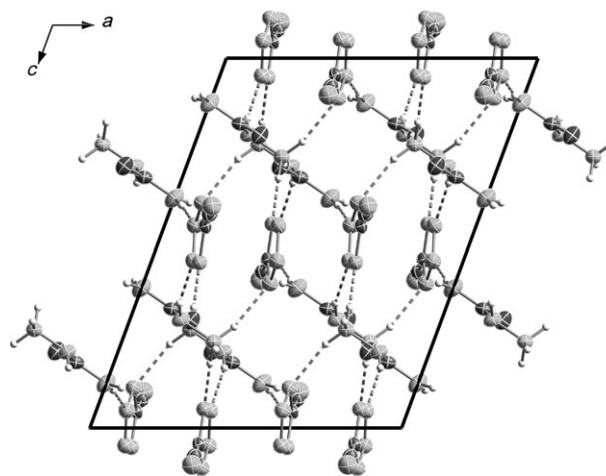


Figure 7. View of the unit cell of **5** along the b axis showing the hydrogen bonding in the structure (dotted lines).

Lastly, five cations coordinate to the anion by forming hydrogen bonds (Supporting Information, Figure 2a). Apart from a very strong hydrogen bond formed between cations ($N8 \cdots O^i = 2.688(2)$ Å; symmetry code: i: $0.5-x, -0.5+y, 0.5-z$), the rest of the interactions are of moderate strength, with distances between donor and acceptor atoms of ≈ 3.0 Å.

Although both the cation and anion in **6** are planar, the compound does not crystallise forming planar layers, because extensive hydrogen bonding is present in the unit cell. As shown in Figure 8, every 5-cyanotetrazolate anion participates in hydrogen bonding to four guanidinium cations. Three of these cations lie on approximately the same plane as the anion, and the fourth one (symmetry code: vii: $1+x, y, z$) is slightly off-plane by $\approx 25^\circ$. Table 4 of the Supporting Information gives a summary of the distances and angles of the hydrogen bonds formed in the crystal structure of the compound. Five medium-to-strong hydrogen bonds are present, with donor-acceptor distances of ≈ 3 Å, and three weaker contacts are also observed with distances of ≈ 3.2 – 3.3 Å. Two of the weak interactions are formed by the same

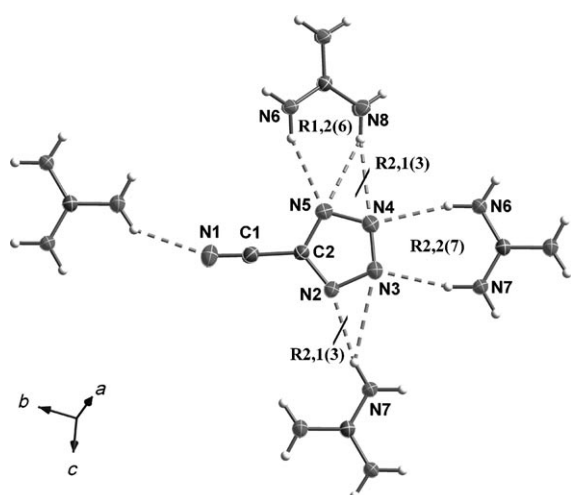


Figure 8. Hydrogen bonding around the anion in **6** showing some characteristic ring graph-sets, and labelling scheme for the anion (diamond plot with thermal ellipsoids at 50% probability).

nitrogen atom of the out-of-plane guanidinium cation ($N8 \cdots N4^i = 3.328(2)$ and $N8 \cdots N5^i = 3.167(2)$ Å; symmetry code: *i*: $-1+x, y, z$).

Compound **9**·H₂O crystallises as a monohydrate with a moderate density of 1.499 g cm^{-3} in a layered structure. In the unit cell there is hydrogen bonding between layers ($N11 \cdots N3 = 3.186(2)$ and $N11 \cdots N4^{iii} = 3.189(2)$ Å; symmetry code: *iii*: $1+x, y, z$). The three NH₂-group lone pairs in the cation (X-ray labels N9, N10, and N11) are involved in the formation of intramolecular hydrogen bonds to the N–H moieties, with donor–acceptor distances of ≈ 2.7 Å. The formation of these intramolecular hydrogen bonds forces the hydrogen atoms of the NH₂ groups to point out of the plane of the cations, allowing the formation of the abovementioned hydrogen bonds between layers. Figure 9 shows the hydrogen bonding around the 5-cyanotetrazolate anion in the crystal structure of **9**·H₂O. In contrast to the guanidinium salt **6**, which forms a strong hydrogen bond by using the

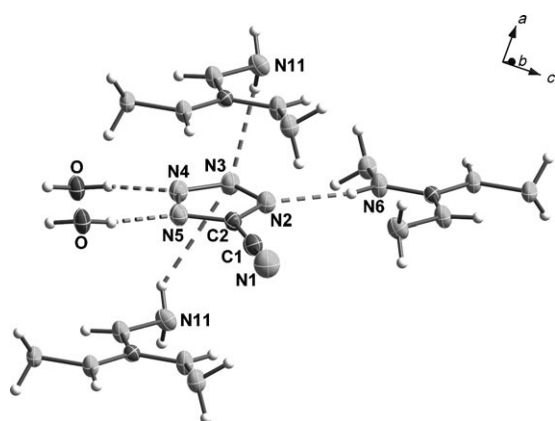


Figure 9. Hydrogen bonding around the anion in **9**·H₂O. The labelling scheme for the anion is shown (diamond plot with thermal ellipsoids at 50% probability).

nitrogen atom of the CN group ($N8 \cdots N1^{iv} = 2.964(2)$ Å; symmetry code: *iv*: $-x, -0.5+y, 0.5-z$), in the triaminoguanidinium compound there are only two very weak “contacts” to this atom ($N9 \cdots N1 = 3.432(2)$ and $N9 \cdots N1^{iii} = 3.364(2)$ Å; symmetry code: *iii*: $1+x, y, z$). All the nitrogen atoms of the tetrazolate ring are involved in the formation of hydrogen bonds. N4 and N5 interact with two water molecules, with O \cdots N distances of ≈ 2.8 Å, N3 forms hydrogen bonds with two cations (interlayer hydrogen bonding), and N2 with one cation ($N6 \cdots N2^i = 2.873(2)$ Å; symmetry code: *i*: $1-x, -y, 1-z$).

Energetic properties: The physical and chemical properties of the 5-cyanotetrazolate salts **1–9** are summarised in Table 3. Differential scanning calorimetry analysis (DSC)

Table 3. Physical and chemical properties of 5-cyanotetrazolate salts **1–9**.

| | 1 ·1.5H ₂ O | 2 | 3 | 4 | 5 |
|--|--|---------------------------------|--|--|--|
| formula | C ₂ H ₃ N ₅ O _{1.5} Na | C ₂ N ₃ K | C ₂ H ₄ N ₆ | C ₂ H ₃ N ₇ | C ₃ H ₆ N ₈ O |
| <i>M_r</i> [g mol ⁻¹] | 144.02 | 132.98 | 112.09 | 127.11 | 170.13 |
| <i>T_m</i> [°C] ^[a] | 275 | 260 | 134 | 138 | 130 |
| <i>T_d</i> [°C] ^[b] | 275 | 265 | 191 | 248 | 140 |
| N [%] ^[c] | 48.6 | 52.6 | 75.0 | 77.1 | 65.9 |
| N + O [%] ^[d] | 65.3 | 52.6 | 75.0 | 77.1 | 75.3 |
| Ω [%] ^[e] | -55.5 | -60.1 | -45.3 | -81.8 | -75.2 |
| ρ [g cm ⁻³] ^[f] | 1.597 | 1.923 | 1.499 | 1.587 ^[f] | 1.521 |
| -Δ <i>U</i> _{comb.} [cal g ⁻¹] ^[g] | - | - | 3565 | 3703 | 3289 |
| Δ <i>U</i> _f ^o [kJ kg ⁻¹] ^[h] | - | - | +2906 | +3795 | +1894 |
| Δ <i>H</i> _f ^o [kJ kg ⁻¹] ^[i] | - | - | +2796 | +3678 | +1784 |

| | 6 | 7 | 8 | 9 ·H ₂ O | 9 |
|--|--|--|---|--|---|
| formula | C ₃ H ₆ N ₈ | C ₃ H ₇ N ₉ | C ₃ H ₈ N ₁₀ | C ₃ H ₁₁ N ₁₁ O | C ₃ H ₉ N ₁₁ |
| <i>M_r</i> [g mol ⁻¹] | 154.13 | 169.15 | 184.16 | 217.19 | 199.18 |
| <i>T_m</i> [°C] ^[a] | 160 | 87 | 123 | 133 | 134 |
| <i>T_d</i> [°C] ^[b] | 210 | 220 | 200 | 178 | 180 |
| N [%] ^[c] | 72.7 | 74.5 | 76.1 | 70.9 | 77.4 |
| N + O [%] ^[d] | 72.7 | 74.5 | 76.1 | 78.3 | 77.4 |
| Ω [%] ^[e] | -93.4 | -89.9 | -86.9 | -77.3 | -84.3 |
| ρ [g cm ⁻³] ^[f] | 1.451 | 1.510 ^[f] | 1.485 ^[f] | 1.499 | 1.512 ^[f] |
| -Δ <i>U</i> _{comb.} [cal g ⁻¹] ^[g] | 3665 | 3702 | 3745 | 4010 | 3835 |
| Δ <i>U</i> _f ^o [kJ kg ⁻¹] ^[h] | +2222 | +2713 | +3173 | +3475 | +3789 |
| Δ <i>H</i> _f ^o [kJ kg ⁻¹] ^[i] | +2110 | +2596 | +3052 | +3361 | +3665 |

[a] Chemical melting point (DSC onset) from measurement with $\beta = 5^\circ \text{C min}^{-1}$. [b] Decomposition point (DSC onset) from measurement with $\beta = 5^\circ \text{C min}^{-1}$. [c] Nitrogen percentage. [d] Combined oxygen and nitrogen contents. [e] Oxygen balance according to reference [27]. [f] Density from X-ray measurements or picnometer. [g] Calculated (MP2 method) constant volume energy of combustion. [h] Calculated (MP2 method) energy of formation. [i] Calculated (MP2 method) enthalpy of formation.

was used to determine the melting and decomposition points of all the materials. The two metal salts in this work (**1**·1.5H₂O and **2**) melt and decompose at temperatures of 275 and 265 °C, respectively. The decomposition points of **1**·1.5H₂O and **2** are significantly higher than those of the sodium and potassium salts of the 5-nitrotetrazolate (200 and 195 °C, respectively)^[9a] and the 5-azidotetrazolate (155 and 148 °C, respectively)^[10] anions, and are comparable to analogous salts containing the 5-aminotetrazolate^[23] or 5-nitriminotetrazolate^[24] anions. The melting points of many of the nitrogen-rich salts (**3–9**) are around 130 °C, and with the

exception of the semicarbazidium salt **5**, which decomposes shortly after melting ($T_d=140^\circ\text{C}$), the nitrogen-rich salts have excellent thermal stabilities ranging from 178 (**9**·H₂O) to 248 °C (**4**), which are clearly distinct from their melting points. It is particularly worth pointing out the low melting point of the aminoguanidinium salt **7** ($T_m=87^\circ\text{C}$), which classifies **7** as an energetic ionic liquid (i.e., melting point below 100 °C), and also its excellent thermal stability of up to 220 °C. This wide liquid range ($\approx 130^\circ\text{C}$) for the aminoguanidinium salt has been noted previously for the analogous salt containing the 5-(5-nitrotetrazol-2-ylmethyl) tetrazolate anion.^[3e]

The nitrogen content, combined nitrogen/oxygen content, oxygen balance,^[27] and density are important physical properties in energetic materials. With the exception of the metal salts **1**·1.5 H₂O and **2**, all the compounds in this study have high nitrogen contents in the range N=66% (**5**) to 77% (**4** and **9**). All the salts have negative oxygen balances between -45% (**3**) and -93% (**6**), comparable to the commonly used high explosive TNT (-74%). The densities of **3–9** range from 1.451 (**6**) to 1.587 g cm⁻³ (**4**), and are lower than those of commonly used high explosives, but higher than those of new-generation nitrogen-rich compounds based on the 5,5'-azotetrazolate anion.^[1j,2a,15]

The values for the heats of combustion for compounds **3–9** were calculated on the basis of the electronic and zero-point energies of the anion and the cations, as described previously (see Experimental Section for a description of the method used in this work).^[8] The energies of formation of all the compounds were then back-calculated on the basis of the general combustion equations for CHNO compounds (see below for the combustion equations of salts **3–9**), Hess's Law, the standard heats of formation for water and carbon dioxide,^[28] and a correction for the change in the gas volume during combustion. The high nitrogen content of compounds **3–9** results in high positive heats of formation. The semicarbazidium salt **5** has the least positive value at +1784 kJ kg⁻¹, and the hydrazinium salt **4** exhibits the largest value at +3678 kJ kg⁻¹. These heats of formation are higher (i.e., more positive) than for TNT and RDX because of the high nitrogen content of the compounds. By using the calculated heats of formation for salts **3–9**, the densities (either from X-ray or picnometer measurements), and the molecular formula, the detonation parameters were calculated using the EXPLO5 computer code.^[29] The results of these calculations are included in Table 4, along with the values of friction and impact sensitivity and the results of the "flame test" (i.e., thermal shock response).

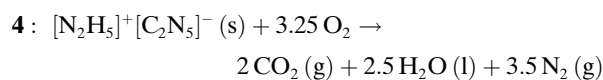
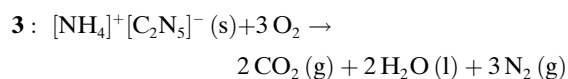
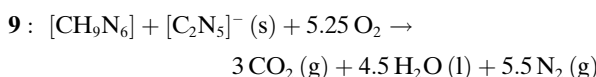
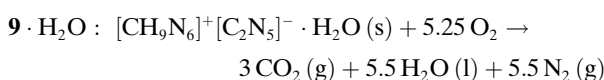
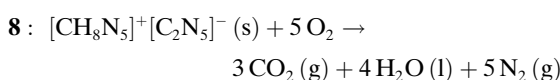
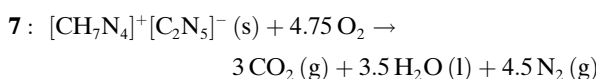
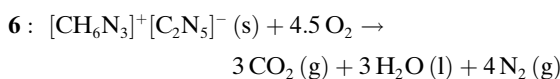
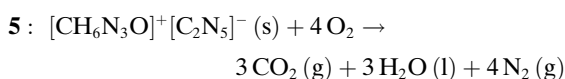


Table 4. Initial safety testing results and predicted energetic performance of 5-cyanotetrazolate salts **1–9**.

| | T_{ex} [K] ^[a] | V_0 [L kg ⁻¹] ^[b] | P_{det} [GPa] ^[c] | D [ms ⁻¹] ^[d] | i [J] ^[e] | f [N] ^[e] | Thermal shock ^[f] |
|--------------------------------|---------------------------------------|---|--|---|---------------------------|---------------------------|------------------------------|
| 1 ·1.5 H ₂ O | – | – | – | – | >40 | >360 | burns |
| 2 | – | – | – | – | >40 | >360 | burns |
| 3 | 2669 | 785 | 19.0 | 7576 | <25 | >360 | burns |
| 4 | 3081 | 818 | 26.7 | 8717 | <15 | <200 | deflagrates |
| 5 | 2812 | 783 | 19.0 | 7451 | >40 | >360 | burns |
| 6 | 2312 | 786 | 15.9 | 7107 | >40 | >360 | burns |
| 7 | 2550 | 811 | 20.1 | 7822 | >40 | >360 | burns |
| 8 | 2769 | 833 | 21.4 | 8059 | <35 | >360 | deflagrates |
| 9 ·H ₂ O | 3312 | 885 | 26.5 | 8817 | >40 | >360 | deflagrates |
| 9 | 3051 | 851 | 25.2 | 8645 | <20 | <300 | deflagrates |

[a] Temperature of the explosion gases. [b] Volume of the explosion gases. [c] Detonation pressure. [d] Detonation velocity. [e] Tests according to BAM methods (see references [31–33]); i =impact, f =friction. [f] Response to fast heating using an open flame.



Looking at the detonation velocities, **3–9** all present higher values than TNT (6881 ms⁻¹), and the hydrazinium (**4**) and triaminoguanidinium (**9**·H₂O and **9**) salts exhibit calculated performances comparable to, or higher than, high-performing, commonly used high explosives such as pentaerythritol tetranitrate (PETN, 8564 ms⁻¹).^[30] Additionally, BAM tests^[31–33] on **4**, **9**·H₂O, and **9** exhibited lower sensitivities towards impact and friction for these three compounds (**4**: $i < 15 \text{ J}$, $f < 200 \text{ N}$; **9**·H₂O: $i > 40 \text{ J}$, $f > 360 \text{ N}$; and **9**: $i < 20 \text{ J}$, $f < 300 \text{ N}$) in comparison to PETN. Apart from the ammonium salt (**3**), which is slightly impact-sensitive ($i < 25 \text{ J}$), the remainder of the compounds, including both metal salts **1**·1.5 H₂O and **2**, are neither impact- nor friction-sensitive ($i > 40 \text{ J}$, $f > 360 \text{ N}$). Lastly, the response to fast heating in the flame (i.e., the thermal shock response) was of normal burning for salts **1**·1.5 H₂O, **2**, **3**, **5**, and **6**, whereas compounds **4**, **8**, **9**·H₂O, and **9** deflagrated. This observation is in agreement with the higher nitrogen and energy content of the last set compounds.

Due to the negative oxygen balances of salts **3–9**, the detonation parameters of mixtures of these compounds with

oxidants such as ammonium nitrate (AN) and ammonium dinitramide (ADN) were predicted using the EXPLO5 code. The formulations were composed of a mixture of the compound and oxidant in approximately neutral oxygen ratios. The results of these calculations are included in the Supporting Information (Tables 9 and 10). By comparing the values of the predicted detonation velocities of compounds **3–9** with those of mixtures with AN (≈ 8000 – 8300 ms^{-1}), higher values are predicted for the formulations with the lower performing salts **3**, **5**, **6**, **7**, and **8**, whereas the more energetic compounds, **4**, **9-H₂O**, and **9**, are expected to be more powerful explosives as the stand-alone materials. However, formulations of all nitrogen-rich salts with ADN ($D \approx 8750$ – 9050 ms^{-1}) are expected to increase the performance significantly in comparison with the pure compounds.

The heats of explosion and gases formed upon decomposition of the nitrogen-rich 5-cyanotetrazolate salts **3–9** were predicted using the ICT code.^[35] These values were calculated by combining the molecular formula of the compounds with their density (either from X-ray or picnometer measurements) and the predicted heats of formation (calculated using quantum chemical methods). The results of these calculations are presented in Table 5 along with the predicted values for the commonly used RDX and TEX for comparison purposes. These calculations predict large amounts of molecular nitrogen being produced upon decomposition of compounds **3–9** (between 555 and 632 g kg^{-1}), as would be expected from nitrogen-rich materials ($66 < N < 77\%$). This is in contrast with the low nitrogen values expected for RDX and TEX (374 and 211 g kg^{-1} , respectively). This observation is in agreement with the fact that nitrogen-rich compounds derive their energy mainly from their high nitrogen content, in contrast to commonly used explosives, which derive their energy from the oxidation of the carbon backbone. In accordance with this last statement, CO_2 is one of the main products expected upon decomposition of RDX and TEX (293 and 405 g kg^{-1} , respectively). As expected, since compounds **3–9** are, with the exception of salts **5** and **9-H₂O**, exclusively based on C, H, and N, no CO_2 production

is predicted for these materials. The low amount of CO_2 expected for **5** (only $< 2 \text{ g kg}^{-1}$) shows that the oxygen in the semicarbazidium cation is expected not to be an oxidant, and to participate mainly in the formation of gaseous water (103 g kg^{-1}). Also, in the hydrate compound **9-H₂O** the oxygen in the molecule is expected to form exclusively gaseous water (82 g kg^{-1}). Due to the negative oxygen balance of salts **3–9**, incomplete combustion is expected, and therefore C soot is also predicted to form in relatively large amounts (between 148 and 204 g kg^{-1}), which are, however, comparable to the value predicted for TEX (152 g kg^{-1}). Due to the high numbers of N–H bonds in compounds **3–9**, NH_3 is calculated to form in relatively large amounts (between 98 and 199 g kg^{-1}); these values increase progressively in the direction from **6** to **9** for the guanidinium salts. Interestingly, highly toxic gases such as CO or HCN are expected to form only in minor amounts for salts **3–9** (CO $< 3 \text{ g kg}^{-1}$, and HCN $< 2 \text{ g kg}^{-1}$), whereas the code predicts larger amounts of CO for the better oxygen-balanced compounds RDX and TEX ($> 20 \text{ g kg}^{-1}$). Lastly, the values of the heats of explosion are relatively high, and that of compound **9-H₂O** (1249 cal g^{-1}) is comparable to that of TEX (1237 cal g^{-1}).

Conclusion

Energetic nitrogen-rich salts based on the 5-cyanotetrazolate anion and ammonium, hydrazinium, semicarbazidium, and guanidinium cations were synthesised in good yields and purities, and characterised by analytical and spectroscopic methods. Wherever possible, the structures of the compounds were determined by X-ray crystallography. The structures of the compounds are described in the formalism of graph-set analysis, which gives information about the types of hydrogen-bonding patterns formed in the solid state. Quantum chemical methods were used to estimate the heats of formation of the new salt-based compounds, and the detonation parameters were predicted using the EXPLO5 computer code. Additionally, the performances of formulations with an oxidiser were also computed. Sensitivity data were obtained experimentally using standard methods, and DSC analysis was used to determine the melting and decomposition points of the new salts. Interestingly, the low melting point of aminoguanidinium compound classifies this salt as an energetic ionic liquid. Furthermore, the ICT code was used to predict the gases formed upon decomposition of the materials. Lastly, the combination of high detonation velocities (comparable to commonly used explosives such as TNT or RDX), with lower sensitivity values (i.e., against impact and friction) than typically used compounds, excellent thermal stabilities, and high nitrogen contents makes the new salts of prospective interest for energetic applications.

Table 5. Predicted decomposition gases and heats of explosion (ICT code)^[a,b] of nitrogen-rich 5-cyanotetrazolate salts **3–9**, and comparison with commonly used high explosives.

| | CO_2 | H_2O | N_2 | CO | H_2 | NH_3 | CH_4 | HCN | C | ΔH_{ex} [cal g^{-1}] ^[c] |
|-------------------------|---------------|----------------------|--------------|------|--------------|---------------|---------------|-----|-------|--|
| 3 | – | – | 631.6 | – | 2.9 | 143.0 | 30.2 | 1.1 | 191.2 | 787 |
| 4 | – | – | 624.3 | – | 2.5 | 178.1 | 21.8 | 1.2 | 172.2 | 1010 |
| 5 | 1.8 | 102.7 | 577.8 | 2.6 | 2.3 | 97.6 | 17.4 | 0.9 | 196.7 | 894 |
| 6 | – | – | 606.6 | – | 3.4 | 145.7 | 39.4 | 1.1 | 203.8 | 634 |
| 7 | – | – | 603.4 | – | 3.1 | 171.7 | 32.2 | 1.1 | 188.4 | 758 |
| 8 | – | – | 610.1 | – | 3.2 | 182.2 | 32.7 | 1.2 | 170.6 | 874 |
| 9-H₂O | – | 81.9 | 554.6 | 1.1 | 2.8 | 187.4 | 22.8 | 1.2 | 147.7 | 1249 |
| 9 | – | – | 609.2 | – | 3.0 | 199.0 | 28.6 | 1.2 | 158.9 | 1027 |
| RDX | 292.6 | 232.8 | 373.9 | 21.5 | 0.2 | 5.1 | – | 0.3 | 72.7 | 1593 |
| TEX ^[d] | 405.4 | 199.8 | 211.4 | 27.5 | 0.2 | 0.3 | – | – | 152.2 | 1237 |

[a] The amount of gas formed at 298 K is given in grams of gas per kilogram of energetic compound. [b] – means the formation of this product was not predicted by the code. [c] Heat of explosion. [d] TEX = 4,10-dinitro-2,6,8,12-tetraoxa-4,10-diazatetrayclododecane.

Experimental Section

Computational methods: The electronic and zero-point energies of the 5-cyanotetrazolate anion and all the cations in salts **3–9** were calculated in order to obtain an estimate of the energy of formation of the compounds in this study. In addition, the vibrational frequencies and corresponding intensities (IR) and activities (Raman) were computed by means of quantum chemical calculations. All calculations were performed by using the Gaussian 03W software package.^[17] For all atoms in all calculations, the correlation-consistent polarised double-basis set cc-pVDZ was used.^[35,36] Electronic and zero-point energies were calculated using Møller–Plesset perturbation theory truncated at the second order (MP2),^[37] and were used unscaled. These values are collected in Table 12 of the Supporting Information. The IR and Raman frequencies of the 5-cyanotetrazolate anion were calculated using Becke’s B3 three-parameter hybrid function with an LYP correlation function (B3LYP),^[38] and were scaled by a factor of 0.9614.^[18] A description of the method used here is given in reference [8].

Cautionary note: Although we did not experience any difficulty when handling the compounds described in this work, tetrazoles are energetic materials and suitable safety precautions need to be taken. It is recommended that laboratories and personnel are properly grounded, and safety equipment, such as Kevlar gloves, leather coats, face shields, and ear plugs, is used.

General procedure: All chemical reagents and solvents of analytical grade were obtained from Sigma–Aldrich Fine Chemicals Inc. and used as supplied. Solvents were dried according to known procedures, freshly distilled, and stored under a nitrogen atmosphere. The ¹H, ¹³C and ¹⁴N NMR spectra were recorded with a JEOL Eclipse 400 instrument, operating at 400.18 MHz (¹H), 100.63 MHz (¹³C), and 40.55 MHz (¹⁴N) in [D₆]DMSO at or near 25 °C. The chemical shifts are given relative to tetramethylsilane (¹H, ¹³C[¹H]) and nitromethane (¹⁴N) as external standards. IR spectra of the solids were recorded on a Perkin–Elmer Spectrum One FTIR instrument as KBr pellets at 25 °C. Raman spectra were recorded on a Perkin–Elmer Spectrum 2000R NIR FT-Raman instrument equipped with a Nd:YAG laser (1064 nm). The intensities are reported relative to the most intense peak and given in parentheses. Elemental analyses were performed with a Netzsch Simultaneous Thermal Analyzer STA 429. Melting points were determined by differential scanning calorimetry (Linseis DSC PT-10 instrument calibrated with standard pure indium and zinc). Measurements were performed in closed aluminium sample pans with a 1 µm hole in the top for gas release, and a 0.003 × 3/16 inch disk was used to optimise the thermal contact between the sample and the container. The nitrogen flow was 20 mL min⁻¹, and an identical empty aluminium sample pan was used as a reference.

Synthesis of sodium 5-cyanotetrazolate monohemihydrate (1.5H₂O): 1.1.5H₂O was synthesised by the [3+2] cycloaddition reaction of NaN₃ and (CN)₂ in liquid SO₂, in analogy to the previously reported caesium salt,^[14] and using the experimental setup presented in the Supporting Information (Figure 1). The solid left in the flask after reaction was dissolved in methanol/water to facilitate its recovery, and the solvent was evaporated. Slow evaporation of a water solution of the compound gave single crystals of 1.5H₂O suitable for X-ray analysis. Elemental analysis calcd (%) for C₂H₃N₅O_{1.5}Na (144.02): C 16.66, H 2.10, N 48.61; found: C 16.42, H 2.04, N 48.42; DSC (5 °C min⁻¹) onset: ≈275 °C (decomp); FAB⁻ (xenon, 6 keV, *m*-NBA matrix): *m/z*: 94.1 [M]⁻; ¹H NMR: δ = 3.35 ppm (s, H₂O); ¹³C[¹H] NMR: δ = 137.7 (1 C; C–CN), 115.1 ppm (1 C; CN); ¹⁴N NMR: δ = 16 (2N; ν_{1/2} = 380 Hz, N3/4), –46 (2N; ν_{1/2} = 400 Hz, N2/5), –119 ppm (1N; ν_{1/2} = 620 Hz, CN); Raman (rel. int.): ν̄ = 2952(6) 2845(4) 2259(65) 1464(5) 1415(100) 1196(12) 1159(4) 1080(42) 1054(11) 1018(8) 739(4) 604(7) 504(15) 215(12) cm⁻¹; IR (KBr, rel. int.): ν̄ = 3519(s) 3413(vs) 3298(s) 2261(m) 1704(w) 1669(w) 1620(vs) 1471(w) 1422(w) 1379(s) 1369(s) 1196(w) 1150(w) 1055(w) 1047(w) 996(w) 752(m) 738(m) 727(m) 659(m) 603(m) 549(s) 533(m) 499(s) cm⁻¹.

Synthesis of potassium 5-cyanotetrazolate (2): Compound **2** was synthesised by the [3+2] cycloaddition reaction of KN₃ and (CN)₂ in liquid SO₂, in analogy to the previously reported caesium salt,^[14] and using the experimental setup presented in Figure 1 of the Supporting Information. Single

crystals of **2** suitable for X-ray analysis were obtained as described for 1.1.5H₂O. Elemental analysis calcd (%) for C₂N₅K (132.98): C 18.05, H –, N 52.65; found: C 17.86, H 0.04, N 52.39; DSC (5 °C min⁻¹) onset: 260 (m.p.), ≈265 °C (decomp); FAB⁻ (xenon, 6 keV, *m*-NBA matrix): *m/z*: 94.1 [M]⁻; ¹³C[¹H] NMR: δ = 137.6 (1 C; C–CN), 115.0 ppm (1 C; CN); ¹⁴N NMR: δ = 18 (2N; ν_{1/2} = 370 Hz, N3/4), –48 (2N; ν_{1/2} = 400 Hz, N2/5), –122 ppm (1N; ν_{1/2} = 610 Hz, CN); Raman (rel. int.): ν̄ = 2264(100) 1418(95) 1178(12) 1135(5) 1096(2) 1074(44) 1048(14) 742(5) 604(12) 501(22) 222(32) 116(9) cm⁻¹; IR (KBr, rel. int.): ν̄ = 2263(s) 1474(w) 1414(m) 1368(vs) 1199(w) 1177(m) 1135(m) 1082(w) 1067(w) 1043(m) 1030(m) 998(w) 974(w) 738(m) 667(w) 603(m) 546(m) 498(s) 439(w) cm⁻¹.

Synthesis of ammonium 5-cyanotetrazolate (3): Sodium 5-cyanotetrazolate monohemihydrate (0.288 g, 2.00 mmol) was dissolved in water (5 mL), and silver nitrate (0.340 g, 2.00 mmol) was added, causing precipitation of the silver salt as a white powder. The suspension was stirred at room temperature and under the exclusion of light for 15 min, and then centrifuged. After decanting the water, the precipitate was washed twice with dry methanol (5 mL). The silver salt was then suspended in dry methanol (5 mL), and ammonium bromide (0.170 g, 1.73 mmol) was added. The reaction mixture was stirred at room temperature for 2 h in the dark, then the insoluble silver bromide was filtered off, and the solution was left to evaporate slowly, resulting in the formation of off-yellow single crystals (used for the X-ray measurements) of compound **3** (0.181 g, 93 %). Elemental analysis calcd (%) for C₂H₄N₆ (112.09): C 21.43, H 3.60, N 74.97; found: C 21.24, H 3.52, N 74.78; DSC (5 °C min⁻¹) onset: 134 (m.p.), ≈191 °C (decomp); FAB⁺ (xenon, 6 keV, *m*-NBA matrix): *m/z*: 18.2 [M]⁺; FAB⁻ (xenon, 6 keV, *m*-NBA matrix): *m/z*: 94.1 [M]⁻; ¹H NMR: δ = 7.09 ppm (s, 4H; NH₄⁺); ¹³C[¹H] NMR: δ = 137.8 (1 C; C–CN), 115.1 ppm (1 C; CN); ¹⁴N NMR: δ = 14 (2N; ν_{1/2} = 390 Hz, N3/4), –46 (2N; ν_{1/2} = 400 Hz, N2/5), –121 (1N; ν_{1/2} = 600 Hz, CN), –359 ppm (1N; ν_{1/2} = 9 Hz, NH₄⁺); Raman (rel. int.): ν̄ = 3079(5) 2880(3) 2821(3) 2272(100) 2217(3) 1890(3) 1416(50) 1186(16) 1135(8) 1080(38) 1048(27) 736(6) 609(12) 501(18) 392(3) 220(14) cm⁻¹; IR (KBr, rel. int.): ν̄ = 3674(w) 3170(s) 3122(s) 3010(s) 2862(m) 2459(w) 2263(s) 2210(w) 2169(w) 2109(w) 2084(w) 1697(w) 1627(w) 1450(vs) 1389(s) 1369(s) 1181(m) 1134(m) 1079(w) 1068(w) 1044(w) 1031(w) 997(w) 833(vw) 737(m) 603(w) 546(m) 497(m) cm⁻¹.

Synthesis of hydrazinium 5-cyanotetrazolate (4): Neat silver nitrate (0.340 g, 2.00 mmol) was added portion-wise to a solution of potassium 5-cyanotetrazolate (0.266 g, 2.00 mmol) in water (5 mL). The reaction mixture was then stirred for 1.5 h in the dark, resulting in the precipitation of silver 5-cyanotetrazolate. The precipitate was centrifuged, and, after removal of the water, was washed twice with dry methanol (2 × 5 mL). Subsequently, the silver salt was suspended in dry methanol (5 mL) and reacted with a solution of hydrazinium bromide (0.192 g, 1.70 mmol) in dry methanol (10 mL). The reaction mixture was stirred for 2 h at room temperature under the exclusion of light, and the insoluble silver bromide was filtered off. The filtrate was then left to evaporate slowly, rendering a slightly yellow powder. This was washed with a solution of diethyl ether/dry methanol (20/1; 10 mL) and dried under vacuum (0.176 g, 81 %). Elemental analysis calcd (%) for C₂H₂N₇ (127.11): C 18.90, H 3.96, N 77.14; found: C 18.78, H 3.87, N 76.81; DSC (5 °C min⁻¹) onset: ≈138 (m.p.), ≈248 °C (decomp); FAB⁺ (xenon, 6 keV, *m*-NBA matrix): *m/z*: 33.2 [M]⁺; FAB⁻ (xenon, 6 keV, *m*-NBA matrix): *m/z*: 94.0 [M]⁻; ¹H NMR: δ = 7.53 ppm (5H; H₂NNH₃⁺); ¹³C[¹H] NMR: δ = 137.8 (1 C; C–CN), 115.1 ppm (1 C; CN); ¹⁴N NMR: δ = 17 (2N; ν_{1/2} = 400 Hz, N3/4), –46 (2N; ν_{1/2} = 420 Hz, N2/5), –117 (1N; ν_{1/2} = 600 Hz, CN), –323 ppm (2N; ν_{1/2} = 800 Hz, H₂NNH₃⁺); Raman (rel. int.): ν̄ = 2259(100) 1620(12) 1522(5) 1418(69) 1184(13) 1142(5) 1099(11) 1082(35) 1049(18) 974(21) 733(5) 602(14) 496(19) 382(3) 311(4) 230(11) cm⁻¹; IR (KBr, rel. int.): ν̄ = 3672(w) 3467(m) 3332(vs) 3281(s) 3241(s) 3071(s) 3016(vs) 2884(s) 2818(s) 2678(s) 2532(m) 2461(m) 2258(s) 2120(m) 2085(m) 2005(w) 1940(w) 1705(w) 1648(m) 1586(s) 1523(vs) 1467(m) 1432(m) 1418(w) 1384(m) 1372(vs) 1275(w) 1238(w) 1183(m) 1142(m) 1119(vs) 1099(s) 1048(w) 1035(w) 975(vs) 810(w) 733(m) 700(w) 599(m) 549(m) 495(m) cm⁻¹.

Synthesis of semicarbazidium 5-cyanotetrazolate (5): A solution of sodium 5-cyanotetrazolate monohydrate (0.288 g, 2.00 mmol) in water (5 mL) was added to solid silver nitrate (0.340 g, 2.00 mmol). The reaction mixture was stirred for 1 h, resulting in the precipitation of the silver salt. The precipitate was then centrifuged, the solvent was decanted, and the solid was washed twice with dry methanol (2×5 mL). At this point silver 5-cyanotetrazolate was suspended in dry methanol (5 mL) and reacted with semicarbazidium hydrochloride (0.165 g, 1.73 mmol) for 2 h at room temperature under the exclusion of light. The insoluble silver chloride was filtered and washed with methanol, and the solvent in the filtrate was left to evaporate slowly. A white powder formed overnight, which was washed with diethyl ether and left to dry in air (0.259 g, 88%). X-ray-quality single crystals were grown by redissolving some of the compound in water and allowing the solvent to evaporate slowly. Elemental analysis calcd (%) for $C_3H_6N_8O$ (170.13): C 21.18, H 3.55, N 65.86; found: C 20.92, H 3.31, N 65.45; DSC ($5^\circ C \text{ min}^{-1}$) onset: ≈ 130 (m.p.), $\approx 140^\circ C$ (decomp); FAB⁺ (xenon, 6 keV, *m*-NBA matrix): *m/z*: 76.1 [*M*]⁺; FAB⁻ (xenon, 6 keV, *m*-NBA matrix): *m/z*: 94.0 [*M*]⁻; ¹H NMR: $\delta = 9.62$ (s, 2H; NH₂⁺), 8.53 (s, 2H; NH₂-CO), 6.54 ppm (s, 2H; NH₂-NH₂⁺); ¹³C{¹H} NMR: $\delta = 157.9$ (1C; C=O), 137.8 (1C; C-CN), 115.1 ppm (1C; CN); ¹⁴N NMR: $\delta = 21$ (2N; $\nu_{1/2} = 390$ Hz, N3/4), -47 (2N; $\nu_{1/2} = 410$ Hz, N2/5), -117 (1N; $\nu_{1/2} = 600$ Hz, CN), -385 ppm (2N; $\nu_{1/2} = 1800$ Hz, NH/NH₂); Raman (rel. int.): $\tilde{\nu} = 2269(100)$, 1688(36), 1624(38), 1600(39), 1531(39), 1422(98), 1268(40), 1193(51), 1144(44), 1081(62), 1051(52), 960(34), 739(38), 708(34), 608(33), 499(43), 383(29), 213(28) cm⁻¹; IR (KBr, rel. int.): $\tilde{\nu} = 3681(w)$, 3408(vs), 3313(s), 3252(s), 3199(s), 2963(s), 2917(s), 2846(s), 2725(s), 2516(m), 2268(m), 2175(w), 2089(w), 1690(vs), 1633(s), 1593(m), 1571(s), 1530(s), 1419(m), 1384(s), 1371(s), 1265(m), 1243(m), 1191(m), 1143(m), 1124(w), 1078(w), 1048(w), 1038(w), 987(w), 961(w), 767(w), 737(w), 697(w), 606(m), 546(m), 517(m), 495(m) cm⁻¹.

Synthesis of guanidinium 5-cyanotetrazolate (6): Guanidinium nitrate (0.244 g, 2.00 mmol) and potassium 5-cyanotetrazolate (0.266 g, 2.00 mmol) were reacted under reflux conditions from pre-dried alcohol (20 mL) for 1 h. Afterwards, potassium nitrate was filtered off and washed with dry methanol. The solvent was removed using a rotary evaporator, and the solid left behind was taken up in a small volume of dry methanol. The methanolic solution was then placed in a diethyl ether chamber overnight, leading to the formation of large single crystals (used for the X-ray measurements) of the compound, which were filtered off and left to dry in air (0.278 g, 90%). Elemental analysis calcd (%) for $C_3H_6N_8$ (154.13): C 23.38, H 3.92, N 72.70; found: C 23.18, H 3.76, N 72.39; DSC ($5^\circ C \text{ min}^{-1}$) onset: ≈ 160 (m.p.), $\approx 210^\circ C$ (decomp); FAB⁺ (xenon, 6 keV, *m*-NBA matrix): *m/z*: 60.1 [*M*]⁺; FAB⁻ (xenon, 6 keV, *m*-NBA matrix): *m/z*: 94.0 [*M*]⁻; ¹H NMR: $\delta = 6.90$ ppm (s, 2H; NH₂⁺); ¹³C{¹H} NMR: $\delta = 157.9$ (1C; C=NH₂⁺), 137.8 (1C; C-CN), 115.1 ppm (1C; CN); ¹⁴N NMR: $\delta = 18$ (2N; $\nu_{1/2} = 380$ Hz, N3/4), -47 (2N; $\nu_{1/2} = 400$ Hz, N2/5), -116 (1N; $\nu_{1/2} = 620$ Hz, CN), -311 ppm (1N; $\nu_{1/2} = 1400$ Hz, NH₂⁺); Raman (rel. int.): $\tilde{\nu} = 3211(1)$ 2263(100) 2209(1) 1682(2) 1662(2) 1587(3) 1563(3) 1472(2) 1420(79) 1379(2) 1368(2) 1190(6) 1153(3) 1079(33) 1057(14) 1051(8) 1013(48) 736(7) 716(1) 607(18) 541(15) 527(5) 497(18) 214(15) 136(8) cm⁻¹; IR (KBr, rel. int.): $\tilde{\nu} = 3674(w)$, 3471(vs), 3377(vs), 3285(s), 3181(s), 2830(w), 2472(w), 2261(m), 2125(vw), 2103(vw), 1665(vs), 1588(m), 1418(w), 1384(m), 1366(s), 1188(w), 1153(m), 1078(w), 1056(w), 1012(w), 735(w), 603(m), 544(m), 496(m) cm⁻¹.

Synthesis of aminoguanidinium 5-cyanotetrazolate (7): Aminoguanidinium nitrate (0.274 g, 2.00 mmol) was dissolved in pre-dried alcohol (20 mL), and reacted with potassium 5-cyanotetrazolate (0.265 g, 2.00 mmol) for 3 h at reflux. The insoluble potassium nitrate was filtered while hot, and the solvent was then removed under vacuum to give an off-white solid, which was extracted with a small volume of dry methanol. After leaving the solvent to evaporate slowly, the product was obtained as a slightly yellow solid (0.330 g, 99%). Elemental analysis calcd (%) for $C_3H_7N_9$ (169.15): C 21.30, H 4.17, N 74.53; found: C 21.08, H 3.90, N 74.01; DSC ($5^\circ C \text{ min}^{-1}$) onset: 87 (m.p.), $\approx 220^\circ C$ (decomp); FAB⁺ (xenon, 6 keV, *m*-NBA matrix): *m/z*: 75.1 [*M*]⁺; FAB⁻ (xenon, 6 keV, *m*-NBA matrix): *m/z*: 94.0 [*M*]⁻; ¹H NMR: $\delta = 8.53$ (s, 1H; NH), 4.66 ppm (2H; NH-NH₂); ¹³C{¹H} NMR: $\delta = 158.8$ (1C; C=NH₂⁺), 137.9 (1C; C-

CN), 115.1 ppm (1C; CN); ¹⁴N NMR: $\delta = 18$ (2N; $\nu_{1/2} = 380$ Hz, N3/4), -48 (2N; $\nu_{1/2} = 400$ Hz, N2/5), -120 (1N; $\nu_{1/2} = 600$ Hz, CN), -319 ppm (2N; $\nu_{1/2} = 1600$ Hz, NH/NH₂); Raman (rel. int.): $\tilde{\nu} = 2263(100)$, 2242(4), 2236(4), 1417(92), 1191(16), 1157(9), 1075(44), 1064(11), 1058(19), 1053(14), 1051(14), 969(20), 736(9), 605(19), 514(15), 494(17), 207(19) cm⁻¹; IR (KBr, rel. int.): $\tilde{\nu} = 3674(w)$, 3454(s), 3345(vs), 3241(s), 3151(s), 2962(m), 2924(m), 2839(w), 2471(w), 2261(m), 2107(w), 1660(s), 1601(m), 1464(w), 1416(w), 1384(m), 1367(m), 1207(w), 1190(w), 1156(w), 1116(w), 1057(w), 1042(w), 974(w), 956(w), 825(vw), 735(w), 654(w), 623(w), 605(w), 546(w), 514(m), 492(m) cm⁻¹.

Synthesis of diaminoguanidinium 5-cyanotetrazolate (8): A solution of potassium 5-cyanotetrazolate (0.22 g, 1.67 mmol) was reacted with a solution of silver nitrate (0.31 g, 1.80 mmol) in water (combined volume ≈ 10 mL). The solution was stirred for 1.5 h under the exclusion of light, and the precipitated silver 5-cyanotetrazolate was centrifuged and washed twice with dry methanol (5 mL). The silver salt was then suspended in dry methanol (10 mL) and reacted with a solution of diaminoguanidinium iodide (0.31 g, 1.43 mmol) in dry methanol (5 mL). Subsequently, the reaction mixture was stirred at room temperature for 2 h in the dark, and the precipitated silver iodide was filtered off and discarded. Compound **8** separated from the solution, upon slow evaporation of the solvent, as a white powder, which was washed with diethyl ether and dried under vacuum (0.221 g, 85%). Elemental analysis calcd (%) for $C_3H_8N_{10}$ (184.16): C 19.57, H 4.38, N 76.06; found: C 19.31, H 4.35, N 74.91; DSC ($5^\circ C \text{ min}^{-1}$) onset: 123 (m.p.), $\approx 200^\circ C$ (decomp); FAB⁺ (xenon, 6 keV, *m*-NBA matrix): *m/z*: 90.1 [*M*]⁺; FAB⁻ (xenon, 6 keV, *m*-NBA matrix): *m/z*: 94.0 [*M*]⁻; ¹H NMR: $\delta = 8.51$ (s, 2H; NH₂⁺), 7.09 (s, 2H; 2 \times NH), 4.57 ppm (s, 4H; 2 \times NH-NH₂); ¹³C{¹H} NMR: $\delta = 159.7$ (1C; C=NH₂⁺), 137.8 (1C; C-CN), 115.1 ppm (1C; CN); ¹⁴N NMR: $\delta = 17$ (2N; $\nu_{1/2} = 400$ Hz, N3/4), -47 (2N; $\nu_{1/2} = 420$ Hz, N2/5), -116 (1N; $\nu_{1/2} = 610$ Hz, CN), -375 ppm (2N; $\nu_{1/2} = 1700$ Hz, NH/NH₂); Raman (rel. int.): $\tilde{\nu} = 2794(23)$, 2775(24), 2734(27), 2710(28), 2256(78), 1983(69), 1415(100), 1186(73), 1149(66), 1067(80), 1054(69), 922(55), 601(39), 498(40), 270(30), 205(29) cm⁻¹; IR (KBr, rel. int.): $\tilde{\nu} = 3659(w)$, 3375(s), 3345(s), 3307(s), 3252(s), 3214(s), 3133(s), 2818(w), 2461(w), 2256(m), 2192(w), 2092(w), 1695(s), 1654(s), 1583(m), 1384(m), 1364(s), 1184(m), 1149(w), 1072(w), 1054(w), 1040(w), 958(m), 924(m), 778(w), 736(w), 669(w), 601(w), 546(w), 497(w) cm⁻¹.

Synthesis of triaminoguanidinium 5-cyanotetrazolate monohydrate (9·H₂O): Potassium 5-cyanotetrazolate (0.265 g, 2.00 mmol) was added to a solution of triaminoguanidinium nitrate (0.334 g, 2.00 mmol) in pre-dried alcohol (20 mL). The solution was heated at reflux for 1 h and the precipitated potassium nitrate was filtered off. The precipitate was washed with dry methanol, then the solvent was evaporated to dryness, and the residue was recrystallised from the minimum amount of water (0.403 g, 93%). Single crystals suitable for X-ray analysis were obtained when an aqueous solution of the compound was left to evaporate slowly at room temperature. Elemental analysis calcd (%) for $C_3H_{11}N_{11}O$ (217.19): C 16.59, H 5.10, N 70.94; found: C 16.37, H 5.42, N 69.96; DSC ($5^\circ C \text{ min}^{-1}$) onset: 82 (-H₂O), 133 (m.p.), 178 $^\circ C$ (decomp); FAB⁺ (xenon, 6 keV, *m*-NBA matrix): *m/z*: 105.1 [*M*]⁺; FAB⁻ (xenon, 6 keV, *m*-NBA matrix): *m/z*: 94.0 [*M*]⁻; ¹H NMR: $\delta = 8.62$ (s, 3H; 3 \times NH), 4.68 ppm (s, 6H; 3 \times NH-NH₂); ¹³C{¹H} NMR: $\delta = 158.9$ (1C; C=NH⁺-NH₂), 137.7 (1C; C-CN), 114.9 ppm (1C; CN); ¹⁴N NMR: $\delta = 17$ (2N; $\nu_{1/2} = 380$ Hz, N3/4), -45 (2N; $\nu_{1/2} = 410$ Hz, N2/5), -118 (1N; $\nu_{1/2} = 610$ Hz, CN), -400 ppm (2N; $\nu_{1/2} = 2000$ Hz, NH/NH₂); Raman (rel. int.): $\tilde{\nu} = 3189(7)$, 2581(8), 2255(65), 1796(17), 1648(18), 1417(64), 1354(21), 1178(26), 1142(24), 1069(44), 1039(31), 886(22), 777(16), 603(23), 544(14), 501(30), 411(17), 272(18), 222(27), 204(19), 188(10), 158(11), 149(11), 130(10), 102(8), 71(7), 56(7) cm⁻¹; IR (KBr, rel. int.): $\tilde{\nu} = 3349$ (m), 3320(m), 3212(s), 3104(m), 3016(w), 2263(m), 2254(m), 2061(w), 1684(s), 1615(m), 1440(w), 1415(w), 1384(m), 1368(m), 1336(m), 1201(w), 1178(w), 1144(m), 1134(m), 1067(w), 984(m), 955(m), 738(w), 637(w), 603(m), 549(w), 498(w) cm⁻¹.

Synthesis of triaminoguanidinium 5-cyanotetrazolate (9): The crystal water in the monohydrated species **9**·H₂O was removed by heating the compound at 60 $^\circ C$ under high vacuum (10^{-3} mbar) for two days, to yield the anhydrous species in quantitative yield. Elemental analysis calcd (%)

for C₃H₉N₁₁ (199.18): C 18.09, H 4.55, N 77.35; found: C 18.03, H 4.34, N 76.89; DSC (5°C min⁻¹) onset: 134 (m.p.), 180°C (decomp); FAB⁺ (xenon, 6 keV, *m*-NBA matrix): *m/z*: 105.1 [M]⁺; FAB⁻ (xenon, 6 keV, *m*-NBA matrix): *m/z*: 94.0 [M]⁻; ¹H NMR: δ = 8.54 (s, 3H; 3×NH), 4.63 ppm (s, 6H; 3×NH–NH₂); ¹³C[¹H] NMR: δ = 158.8 (1C; C=NH⁺–NH₂), 137.7 (1C; C–CN), 115.0 ppm (1C; CN); ¹⁴N NMR: δ = 18 (2N; ν_{1/2} = 380 Hz, N3/4), –43 (2N; ν_{1/2} = 400 Hz, N2/5), –119 (1N; ν_{1/2} = 600 Hz, CN), –397 ppm (2N; ν_{1/2} = 2000 Hz, NH/NH₂); Raman (rel. int.): ν̄ = 3182(4), 2585(5), 2253(54), 1792(12), 1647(15), 1418(71), 1352(14), 1177(25), 1140(17), 1070(51), 1032(11), 891(11), 778(19), 607(28), 547(9), 498(41), 410(12), 272(22), 228(28), 208(18), 151(8), 133(14), 101(7), 69(9) cm⁻¹; IR (KBr, rel. int.): ν̄ = 3208(s), 3100(m), 2255(m), 2060(w), 1685(s), 1615(m), 1440(w), 1411(w), 1383(m), 1371(m), 1337(m), 1187(w), 1145(m), 1131(m), 1068(w), 985(m), 956(m), 735(w), 639(w), 608(m), 508(w), 501(w) cm⁻¹.

Acknowledgements

Financial support of this work by the Ludwig-Maximilian University of Munich (LMU), the Deutsche Forschungsgemeinschaft (DFG CR138/2-1), the U.S. Army Research Laboratory (ARL), the Armament Research, Development and Engineering Center (ARDEC), the Strategic Environmental Research and Development Program (SERDP), and the Office of Naval Research (ONR Global, title: “Synthesis and Characterization of New High Energy Dense Oxidizers (HEDO) - NICOP Effort”) under contract nos. W911NF-09-2-0018 (ARL), W911NF-09-1-0120 (ARDEC), W011NF-09-1-0056 (ARDEC) and 10 WPSEED01-002/WP-1765 (SERDP) is gratefully acknowledged. The authors acknowledge collaborations with Dr. Mila Krupka (OZM Research, Czech Republic) in the development of new testing and evaluation methods for energetic materials, and with Dr. Muhamed Suscesa (Brodarski Institute, Croatia) in the development of new computational codes to predict the detonation and propulsion parameters of novel explosives. We are indebted to and thank Dr. Betsy M. Rice and Dr. Brad Forch (ARL, Aberdeen, Proving Ground, MD) and Mr. Gary Chen (ARDEC, Picatinny Arsenal, NJ) for many helpful and inspired discussions and support of our work, as well as the GDCh.

- [1] a) R. P. Singh, R. D. Verma, D. T. Meshri, J. M. Shreeve, *Angew. Chem.* **2006**, *118*, 3664–3682; *Angew. Chem. Int. Ed.* **2006**, *45*, 3584–3601; b) T. M. Klapötke, C. Miró Sabaté, *Z. Anorg. Allg. Chem.* **2007**, *633*, 2671–2677; c) R. Wang, H. Gao, C. Ye, B. Twamley, J. M. Shreeve, *Inorg. Chem.* **2007**, *46*, 932–938; d) Y. Guo, H. Gao, B. Twamley, J. M. Shreeve, *Adv. Mater.* **2007**, *19*, 2884–2888; e) H. Xue, H. Gao, B. Twamley, J. M. Shreeve, *Chem. Mater.* **2007**, *19*, 1731–1739; f) Z. Zeng, H. Gao, B. Twamley, J. M. Shreeve, *J. Mater. Chem.* **2007**, *17*, 3819–3826; g) Y. Gao, H. Gao, C. Piekarski, J. M. Shreeve, *Eur. J. Inorg. Chem.* **2007**, 4965–4972; h) C. Darwich, T. M. Klapötke, C. Miró Sabaté, *Chem. Eur. J.* **2008**, *14*, 5756–5771; C. Miró Sabaté, *Propellants Explos. Pyrotech.* **2008**, *33*, 336–346; i) T. M. Klapötke, C. Miró Sabaté, *Chem. Mater.* **2008**, *20*, 1750–1763.
- [2] a) T. M. Klapötke, C. Miró Sabaté, *Chem. Mater.* **2008**, *20*, 3629–3637; b) C. Darwich, T. M. Klapötke, C. Miró Sabaté, *Chem. Eur. J.* **2008**, *14*, 5756–5771; c) T. M. Klapötke, C. Miró Sabaté, J. Stierstorfer, *Z. Anorg. Allg. Chem.* **2008**, *634*, 1867–1874; d) M. von Denffer, T. M. Klapötke, C. Miró Sabaté, *Z. Anorg. Allg. Chem.* **2008**, *634*, 2575–2582; C. Miró Sabaté, *Z. Anorg. Allg. Chem.* **2008**, *634*, 2575–2582; e) T. M. Klapötke, C. Miró Sabaté, *Eur. J. Inorg. Chem.* **2008**, 5350–5366; f) K. Karaghiosoff, T. M. Klapötke, C. Miró Sabaté, *Chem. Eur. J.* **2009**, *15*, 1164–1176; g) Y.-H. Joo, B. Twamley, S. Garg, J. M. Shreeve, *Angew. Chem.* **2008**, *120*, 6332–6335; *Angew. Chem. Int. Ed.* **2008**, *47*, 6236–6239; h) T. Abe, G.-H. Tao, Y.-H. Joo, Y. Huang, B. Twamley, J. M. Shreeve, *Angew. Chem.* **2008**, *120*, 7195–7198; *Angew. Chem. Int. Ed.* **2008**, *47*, 7087–7090; i) Y.-H. Joo, J. M. Shreeve, *Org. Lett.* **2008**, *10*, 4665–4667; j) R. Wang, Y. Guo, Z. Zeng, D. A. Parrish, B. Twamley, J. M. Shreeve, *Chem. Eur. J.* **2009**, *15*, 2625–2634; k) Y.-H. Joo, D. A. Parrish, J. M. Shreeve, *Angew. Chem.* **2009**, *121*, 572–575; *Angew. Chem. Int. Ed.* **2009**, *48*, 564–567; l) Y.-H. Joo, J. M. Shreeve, *Chem. Eur. J.* **2009**, *15*, 3198–3203; m) T. Abe, Y.-H. Joo, G.-H. Tao, J. M. Shreeve, *Chem. Eur. J.* **2009**, *15*, 4102–4110; n) R. Wang, Y. Guo, Z. Zeng, J. M. Shreeve, *Chem. Commun.* **2009**, 2697–2699; o) Y.-H. Joo, J. M. Shreeve, *Eur. J. Inorg. Chem.* **2009**, 3573–3578.
- [3] a) K. Karaghiosoff, T. M. Klapötke, C. Miró Sabaté, *Eur. J. Inorg. Chem.* **2009**, 238–250; b) T. M. Klapötke, C. Miró Sabaté, M. Rasp, *Dalton Trans.* **2009**, 1825–1834; c) M. Eberspächer, T. M. Klapötke, C. Miró Sabaté, *Helv. Chim. Acta* **2009**, *92*, 977–996; d) M. Eberspächer, T. M. Klapötke, C. Miró Sabaté, *New J. Chem.* **2009**, *33*, 517–527; e) T. M. Klapötke, C. Miró Sabaté, M. Rasp, *J. Mater. Chem.* **2009**, *19*, 2240–2252; f) Y. H. Joo, B. Twamley, J. M. Shreeve, *Chem. Eur. J.* **2009**, *15*, 9097–9104; g) X. Li, D. W. Bruce, J. M. Shreeve, *J. Mater. Chem.* **2009**, *19*, 8232–8238; h) Z. Zeng, Y. Guo, B. Twamley, J. M. Shreeve, *Chem. Commun.* **2009**, 6014–6016; i) G.-H. Tao, B. Twamley, J. M. Shreeve, *Inorg. Chem.* **2009**, *48*, 9918–9923; j) Y. Guo, G.-H. Tao, Z. Zeng, H. Gao, J. M. Shreeve, *Chem. Eur. J.* **2010**, *16*, 3753–3762; k) G.-H. Tao, Y. Guo, D. A. Parrish, J. M. Shreeve, *J. Mater. Chem.* **2010**, *20*, 2999–3005.
- [4] V. A. Ostrovskii, M. S. Pevzner, T. P. Kofman, M. B. Shcherbinin I. V. Tseliniskii, *Targets Heterocycl. Syst.* **1999**, *3*, 467–526.
- [5] a) S. V. Levchik, A. I. Balabanovich, O. A. Ivashkevich, A. I. Lesnikovich, P. N. Gaponik, L. Costa, *Thermochim. Acta* **1992**, *207*, 115; b) S. V. Levchik, A. I. Balabanovich, O. A. Ivashkevich, A. I. Lesnikovich, P. N. Gaponik, L. Costa, *Thermochim. Acta* **1993**, *225*, 53; c) A. I. Lesnikovich, O. A. Ivashkevich, S. V. Levchik, A. I. Balabanovich, P. N. Gaponik, A. A. Kulak, *Thermochim. Acta* **2002**, *388*, 233; d) A. Gao, Y. Oyumi, T. B. Brill, *Combust. Flame* **1991**, *83*, 345; e) S. V. Levchik, A. I. Balabanovich, O. A. Ivashkevich, P. N. Gaponik, L. Costa, *Polym. Degrad. Stab.* **1995**, *47*, 333.
- [6] a) G.-H. Tao, Y. Guo, Y.-H. Joo, B. Twamley, J. M. Shreeve, *J. Mater. Chem.* **2008**, *18*, 5524–5530; b) T. M. Klapötke, C. Miró Sabaté, *Z. Anorg. Allg. Chem.* **2009**, *635*, 1812–1822; c) T. M. Klapötke, C. Miró Sabaté, A. Penger, J. M. Welch, *Eur. J. Inorg. Chem.* **2009**, 880–896; d) K. Karaghiosoff, T. M. Klapötke, P. Mayer, C. Miró Sabaté, A. Penger, J. M. Welch, *Inorg. Chem.* **2008**, *47*, 1007–1019; C. Miró Sabaté, A. Penger, J. M. Welch, *Inorg. Chem.* **2008**, *47*, 1007–1019; e) T. M. Klapötke, C. Miró Sabaté, M. Rusan, *Z. Anorg. Allg. Chem.* **2008**, *634*, 688–695.
- [7] T. M. Klapötke, C. Miró Sabaté, J. Stierstorfer, *New J. Chem.* **2009**, *33*, 136–147.
- [8] T. M. Klapötke, P. Mayer, C. Miró Sabaté, J. M. Welch, N. Wiegand, *Inorg. Chem.* **2008**, *47*, 6014–6027.
- [9] a) T. M. Klapötke, C. Miró Sabaté, J. M. Welch, *Dalton Trans.* **2008**, 6372–6380; b) M. H. V. Huynh, M. A. Hiskey, T. J. Meyer, M. Wetzler, *Proc. Natl. Acad. Sci. USA* **2006**, *103*, 5409–5412; c) M. H. V. Huynh, M. D. Coburn, T. J. Meyer, M. Wetzler, *Proc. Natl. Acad. Sci. USA* **2006**, *103*, 10322–10327; d) T. M. Klapötke, C. Miró Sabaté, *Cent. Eur. J. Energ. Mater.* **2010**, *7*, 161–173; e) T. M. Klapötke, C. Miró Sabaté, J. M. Welch, *Heteroat. Chem.* **2009**, *20*, 35–44; f) T. M. Klapötke, C. Miró Sabaté, *Dalton Trans.* **2009**, 1835–1841; g) T. M. Klapötke, C. Miró Sabaté, J. M. Welch, *Eur. J. Inorg. Chem.* **2009**, 769–776.
- [10] T. M. Klapötke, J. Stierstorfer, *J. Am. Chem. Soc.* **2009**, *131*, 1122–1134.
- [11] B. C. Tappan, A. N. Ali, S. F. Son, T. B. Brill, *Propellants Explos. Pyrotech.* **2006**, *31*, 163.
- [12] E. Oliveri-Mandala, T. Passalacqua, *Gazz. Chim. Ital.* **1912**, *41*, 430–435.
- [13] P. L. Franke, W. L. Groeneveld, *Transition Met. Chem.* **1980**, *5*, 240–244.
- [14] H. P. H. Arp, A. Decken, J. Passmore, D. J. Wood, *Inorg. Chem.* **2000**, *39*, 1840–1848.
- [15] a) A. Hammerl, M. Hiskey, G. Holl, T. M. Klapötke, K. Polborn, J. Stierstorfer, J. J. Weigand, *Chem. Mater.* **2005**, *17*, 3784–3793;

- b) T. M. Klapötke, C. Miró Sabaté, *New J. Chem.* **2009**, 33, 1605–1617.
- [16] N. B. Colthup, L. H. Daly, S. E. Wiberley in *Introduction to Infrared and Raman Spectroscopy*, 3rd ed., Academic Press, Boston, **1990**.
- [17] Gaussian 03, Revision A.1: M. J. Frisch, G. W. Trucks, H. B. Schlegel, G. E. Scuseria, M. A. Robb, J. R. Cheeseman, J. A. Montgomery, Jr., T. Vreven, K. N. Kudin, J. C. Burant, J. M. Millam, S. S. Iyengar, J. Tomasi, V. Barone, B. Mennucci, M. Cossi, G. Scalmani, N. Rega, G. A. Petersson, H. Nakatsuji, M. Hada, M. Ehara, K. Toyota, R. Fukuda, J. Hasegawa, M. Ishida, T. Nakajima, Y. Honda, O. Kitao, H. Nakai, M. Klene, X. Li, J. E. Knox, H. P. Hratchian, J. B. Cross, C. Adamo, J. Jaramillo, R. Gomperts, R. E. Stratmann, O. Yazyev, A. J. Austin, R. Cammi, C. Pomelli, J. W. Ochterski, P. Y. Ayala, K. Morokuma, G. A. Voth, P. Salvador, J. J. Dannenberg, V. G. Zakrzewski, S. Dapprich, A. D. Daniels, M. C. Strain, O. Farkas, D. K. Malick, A. D. Rabuck, K. Raghavachari, J. B. Foresman, J. V. Ortiz, Q. Cui, A. G. Baboul, S. Clifford, J. Cioslowski, B. B. Stefanov, G. Liu, A. Liashenko, P. Piskorz, I. Komaromi, R. L. Martin, D. J. Fox, T. Keith, M. A. Al-Laham, C. Y. Peng, A. Nanayakkara, M. Challacombe, P. M. W. Gill, B. Johnson, W. Chen, M. W. Wong, C. Gonzalez, J. A. Pople, Gaussian, Inc. Pittsburgh PA, **2004**.
- [18] A. P. Scott, L. Radom, *J. Phys. Chem.* **1996**, 100, 16502–16513.
- [19] G. M. Sheldrick, SHELXS-97, Program for Crystal Structure Solution, Universität Göttingen, Germany, **1997**.
- [20] G. M. Sheldrick, SHELXL-97, Program for the Refinement of Crystal Structures, Universität Göttingen, Germany, **1997**.
- [21] L. J. Farrugia, *J. Appl. Crystallogr.* **1999**, 32, 837–838.
- [22] A. L. Speck, Platon; Utrecht University: Utrecht, The Netherlands, **1999**.
- [23] V. Ernst, T. M. Klapötke, J. Stierstorfer, *Z. Anorg. Allg. Chem.* **2007**, 633, 879–887.
- [24] T. M. Klapötke, H. Radies, J. Stierstorfer, *Z. Naturforsch.* **2007**, 62b, 1343–1352.
- [25] J. H. Huheey, *Inorganic Chemistry: Principles of Structure and Reactivity*, 3rd ed., Harper and Row, New York, **1983**.
- [26] A. F. Hollemann, E. Wieberg, N. Wieberg in *Lehrbuch der Anorganischen Chemie*, 101th ed., Gruyter, Berlin, **1995**.
- [27] Oxygen balance for a compound with the formula $C_xH_yO_zM_t$: Ω (%): $-1600(2x+y/2+t-z)/MW$; where M is a metal and MW is the molecular weight.
- [28] NIST Chemistry WebBook, NIST Standard Reference Database Number 69, **2003**, www version: <http://webbook.nist.gov/chemistry>.
- [29] a) M. Suceca, *Propellants Explos. Pyrotech.* **1991**, 16, 197; b) M. Suceca, *Propellants Explos. Pyrotech.* **1999**, 24, 280.
- [30] J. Köhler, R. Mayer *Explosivstoffe*, 9th ed., Wiley-VCH, Weinheim, **1998**.
- [31] UN Recommendations on the Transport of Dangerous Goods: Impact: Insensitive > 40 J, less sensitive ≥ 35 J, sensitive ≥ 4 J, very sensitive ≤ 3 J. Friction: Insensitive > 360 N, less sensitive 360 N, sensitive < 360 N and > 80 N, very sensitive ≤ 80 N, extremely sensitive ≤ 10 N.
- [32] a) NATO standardisation agreement (STANAG) on explosives, impact sensitivity tests, no. 4489, Ed. 1, Sept. 17, **1999**; b) NATO standardisation agreement (STANAG) on explosive, friction sensitivity tests, no. 4487, Ed. 1, Aug. 22, **2002**.
- [33] a) WIWEB-Standardarbeitsanweisung 4–5.1.02, Ermittlung der Explosionsgefährlichkeit, hier der Schlagempfindlichkeit mit dem Fallhammer, Nov. 8, **2002**; b) WIWEB-Standardarbeitsanweisung 4–5.1.03, Ermittlung der Explosionsgefährlichkeit oder der reibeempfindlichkeit mit dem Reibeapparat, Nov. 8, **2002**.
- [34] a) ICT-Thermodynamic Code, Version 1.0, Fraunhofer-Institut für Chemische Technologie, Pfingsttal, Germany, **1988–2000**; b) R. Webb, M. van Rooijen, *Proceedings of the 29th International Pyrotechnics Seminar*, Westminster, CO, **2002**.
- [35] R. A. Kendall, T. H. Dunning, R. J. Harrison, *J. Chem. Phys.* **1992**, 96, 6796–6806.
- [36] K. A. Peterson, D. E. Woon, T. H. Dunning, *J. Chem. Phys.* **1994**, 100, 7410–7415.
- [37] J. A. Pople, R. Seeger, R. Krishnan, *Int. J. Quantum Chem. Symp.* **1977**, 11, 149–163.
- [38] B. Michlich, A. Savin, H. Stoll, H. Preuss, *Chem. Phys. Lett.* **1989**, 157, 200–206.

Received: July 28, 2010
Published online: December 15, 2010